Demagnetizing Factors for Cylinders

Du-Xing Chen, James A. Brug, *Member, IEEE,* and Ronald B. Goldfarb, *Senior Member, IEEE*

***Abstract*—Fluxmetric (ballistic) and magnetometric demagnetizing factors N_f and N_m for cylinders as functions of susceptibility χ and the ratio γ of length to diameter have been evaluated. Using a one-dimensional model when $\gamma \geq 10$, N_f was calculated for $-1 \leq \chi < \infty$ and N_m was calculated for $\chi \to \infty$. Using a two-dimensional model when $0.01 \leq \gamma \leq 50$, an important range for magnetometer measurements, N_m and N_f were calculated for $-1 \leq \chi < \infty$. Demagnetizing factors for $\chi < 0$ are applicable to superconductors. For $\chi = 0$, suitable for weakly magnetic or saturated ferromagnetic materials, N_f and N_m were computed exactly using inductance formulas.**

I. Introduction

THE study of demagnetizing factors for ellipsoids and their degenerate forms (spheres, infinite plates, infinite cylinders) dates from the work of Poisson [1] and was elaborated upon by Thomson [2], Evans and Smith [3], and Maxwell [4]. Experimental investigations on finite right circular cylinders began in the 1870's, when ballistic galvanometers were first used in magnetic measurements of iron [5], [6]. The literature distinguishes between "magnetometric" and "fluxmetric" (or "ballistic") demagnetizing factors N_m and N_f [7]. N_m refers to an average of magnetization over the entire specimen and is appropriate for magnetometer measurements of small samples. N_f refers to an average of magnetization at the midplane of the sample and is appropriate for measurements made with short search coils. Values of the demagnetizing factor were deduced from the shearing of the magnetic hysteresis loop [8], a procedure originally developed by Lord Rayleigh for ellipsoids [9], or by measuring the magnetization and the field at the cylinder's side [10]. Factors for cylinders of several aspect ratios were published [7], [8], [11], [12]. By the 1900's, it was apparent that the values of the factors depended on the susceptibility χ of the material [13]–[15].

Although it has been criticized from a pedagogical point of view [16], [17], the use of fictitious magnetic poles to calculate demagnetizing fields has been universal. The first theoretical treatment of magnetic pole distributions in finite cylinders was by Green [18]. An early model to attempt to explain experimental data considered point magnetic poles at each end of a cylinder [19]. This simplistic model could be used only for long uniformly magnetized cylinders, and the results deviated significantly from experimental data on ferromagnetic samples. During the 1920's and 1930's, there were several theoretical papers on N_f for material with constant susceptibility χ. The results were given as functions of χ and the length-to-diameter ratio γ. These used one-dimensional models with approximations as needed to suit the computational techniques of the time. The first systematic theoretical calculation of N_f for the high susceptibility case was done by Würschmidt [20], [21]. He calculated N_f of cylinders using a one-dimensional model in which the cylinder had side surface poles and point end poles. He used Taylor expansions for the magnetization and the demagnetizing field at the midplane. The calculation was complicated, and he completed it only for the case $\gamma = 50$ and $\chi \to \infty$. For the γ and χ dependence of N_f, he gave qualitative results using the first few terms of the expansion. A similar approach with simpler expressions was used by Neumann and Warmuth [22], who calculated N_f for $\chi \to \infty$ and $\gamma \geq 10$.

To obtain the susceptibility dependence of N_f, Stäblein and Schlechtweg [23] used a quadratic approximation and two linear differential equations. The model was improved by substituting uniform end-surface poles for point end poles. Their results included 30 values of N_f for $10 \leq \gamma \leq 500$ and $12.56 \leq \chi < \infty$. An extension of the γ region to 0 was achieved by Warmuth [24]–[26], who fitted existing data and extrapolated graphically using the demagnetizing factor N of ellipsoids as a reference. The values of N_f calculated from the one-dimensional models were consistent with the data of ballistic measurements on soft magnetic materials. Bozorth and Chapin [27] compiled the results, which were later plotted in Bozorth's book [28].

To obtain axial demagnetizing factors more accurately, especially for short cylinders, two-dimensional calculations are needed. The simplest case is $\chi = 0$, where N_m and N_f as functions of γ can be derived analytically. The approximation $\chi = 0$ applies to diamagnets, paramagnets, and saturated ferromagnets. N_m for 25 values of γ from 0.2 to 1000 were obtained accurately to four significant figures by Brown [29] from a calculation of self-inductance [30] and listed as a table in Brown's book [31]. Crabtree [32] obtained the same values for the average demagnetizing factor by integration of the local field over the cylindrical volume. Moskowitz *et al.* extended

Manuscript received March 11, 1991.

The authors are with the Electromagnetic Technology Division, National Institute of Standards and Technology, Boulder, CO 80303.

D.-X. Chen is on leave from the Electromagnetism Group, Physics Department, Universitat Autònoma de Barcelona, 08193 Bellaterra, Spain.

J. A. Brug is on leave from the Thin Film Department, Hewlett-Packard Laboratories, Palo Alto, CA 94303.

IEEE Log Number 9102083.

Brown's method to cylinders of polygonal cross section [33], and Kaczér and Klem extended it to hollow cylinders [34]. N_f for $\chi = 0$ was calculated exactly by Joseph [35]. Approximate values for N_m and N_f for $\chi = 0$, accurate for large γ, were calculated by Vallabh Sharma using uniformly magnetized volume elements [36]. Sato and Ishii [37] obtained a simple expression to approximate N_m for $\chi = 0$. Chen and Li [38], [39] obtained N_f for $\chi = 0$ using magnetostatic potential calculations.

The susceptibilities $\chi = -1$ and $\chi \to \infty$ correspond to perfectly diamagnetic and ideally soft ferromagnetic materials, respectively. N_m and N_f for these susceptibilities were first treated by Taylor for perfectly conducting cylinders [40], [41]. He developed a method introduced by Smythe that expressed charge densities on the side and ends in terms of a set of orthogonal polynomials, and expanded the electrostatic potential at the cylinder center [42]–[44]. Taylor calculated electric and magnetic polarizabilities for conducting cylinders for $0.25 \leq \gamma \leq 4$ in both the longitudinal and transverse directions. $N_m(\infty)$ can be deduced from his electric polarizability results because of the analogy between electrostatics and magnetostatics. Because his calculation for magnetic polarizability was for a uniform quasi-static but nonpenetrating applied field, $N_m(-1)$ can also be deduced from his results. According to Taylor, his convergence error was less than 0.1% for the longitudinal direction.

Using a similar approach with simpler base functions, Templeton *et al.* calculated axial N_f for $\chi \to \infty$ for $0.05 \leq \gamma \leq 250$ [45], [46]. The fact that the side and end-pole densities have basically a $\delta^{-1/3}$ dependence, where δ is the distance from the corner, was used to construct the set of polynomials. To estimate their error, Templeton and Arrott calculated the root-mean-square deviation of the normalized potential from 0 and found it to be less than 0.31% [45]. Compared to an approximate formula with 8 adjustable parameters, the deviations of their 12 computed $N_f(\infty)$ values were less than 0.25%. The work was based on their earlier magnetostatic analysis of the magnetization process in soft ferromagnetic cylinders with constant end-pole densities [47], [48]. The details of the calculation were published by Aharoni, who also calculated the self-energy of cylinders [49], and more generally, cylinders with nonuniform magnetization [50].

For susceptibilities other than 0, -1, and ∞, different techniques have been used. Archer and Guancial [51] and Fawzi *et al.* [52] calculated the distribution of magnetization and magnetic field in long cylinders with large susceptibilities using volume and boundary integral equations. Using experimental resistance network analogs, Okoshi [53] obtained N_f for $\chi \to \infty$, and Yamamoto and Yamada [54] obtained N_f and N_m for large χ.

Several papers have treated demagnetizing factors at points. Joseph and Schlömann [55] solved for local demagnetizing factors in uniformly magnetized cylinders and used a series expansion to account for nonuniform magnetization. Kraus [56] determined the complete local demagnetizing tensor for uniformly magnetized cylinders. Brug and Wolf [57] calculated the magnetization distribution in disks and obtained the local demagnetizing factor for materials that undergo phase transitions.

In Zijlstra's book [58], N_f and N_m are plotted. These types of graphs and tables appear in other books on magnetism and magnetic materials, and they are widely used, sometimes inappropriately, in magnetic measurements of ferromagnetic, ferrimagnetic, weakly magnetic, and superconducting materials. However, there remain some problems. For $\chi = 0$, the most accurate case, the number of γ values for N_m and N_f is insufficient for accurate interpolation. For $\chi \neq 0$, almost all books give results obtained before 1950, and there are no data for $\chi < 0$. For long cylinders ($\gamma > 10$), there is a lack of data on the χ dependence of N_f, and there are no data on N_m. For short cylinders ($\gamma < 10$), there are even less data, and those that exist have large errors because they were obtained by extrapolation. In summary, there is no complete picture for the γ and χ dependence of N_f and N_m.

In this paper, we calculate N_f and N_m for a complete range of γ and χ. Susceptibility χ is traditionally assumed to be constant in the material and is therefore defined as M/H, where M is the magnetic moment per unit volume and H is the internal magnetic field. For the case $\chi = 0$, in which the magnetization is uniform, we give 61 exact inductance calculations of N_m and N_f for $10^{-5} \leq \gamma \leq 10^3$. For $\chi \neq 0$, more elaborate methods are used. For $\gamma > 10$, the variation of magnetization across the radius of the cylinder is negligible at the midplane, and we calculate N_f as a function of γ and χ ($-1 \leq \chi < \infty$) based on the one-dimensional model of Stäblein and Schlechtweg [23]. Unlike them, we use Taylor expansions for $M(z)$, calculate the demagnetizing field $H_d(z)$ directly at 25 points along the axis, and obtain more accurate results. The model is also applicable to N_m for $\chi \to \infty$. For $0.01 \leq \gamma \leq 50$, a two-dimensional finite element method is used that takes into account the variation of magnetic pole density along the side and ends of the cylinder. Values of N_m and N_f are given for $-1 \leq \chi < \infty$.

II. Fluxmetric and Magnetometric Demagnetizing Factors

The demagnetizing correction is nontrivial for samples in open magnetic circuits. An exact correction can be obtained only for ellipsoids [4], [59], [60], where both the magnetization $\boldsymbol{M}$ and the demagnetizing field $\boldsymbol{H}_d$ are uniform under a uniform applied field $\boldsymbol{H}_a$. If the three principal ellipsoid axes coincide with the x, y, and z axes, the internal field is

$$\boldsymbol{H} = \boldsymbol{H}_a + \boldsymbol{H}_d = \boldsymbol{H}_a - \tilde{N}\boldsymbol{M}, \tag{1}$$

where $\tilde{N}$ is the demagnetizing tensor,

$$\tilde{N} = \begin{bmatrix} N_x & 0 & 0 \\ 0 & N_y & 0 \\ 0 & 0 & N_z \end{bmatrix}, \tag{2a}$$

with

$$N_x + N_y + N_z = 1. \tag{2b}$$

If the applied field is along one of the principal axes, we have

$$\boldsymbol{H} = \boldsymbol{H}_a + \boldsymbol{H}_d = \boldsymbol{H}_a - N\boldsymbol{M}, \tag{3}$$

where N is called the demagnetizing factor. In SI units, $0 \leq N \leq 1$. In cylindrical samples, which are commonly used in magnetic measurements, the demagnetizing field is not uniform, and two kinds of susceptibility-dependent demagnetizing factors are defined.

If the sample is located in a uniform applied field H_a along its axis, the fluxmetric (or ballistic) demagnetizing factor N_f is defined as the ratio of the average demagnetizing field to the average magnetization at the midplane perpendicular to the axis. The magnetometric demagnetizing factor N_m is defined as the ratio of the average demagnetizing field to the average magnetization of the entire sample [58]:

$$\int_S H_d \, ds = -N_f \int_S M \, ds, \tag{4}$$

$$\int_V H_d \, dv = -N_m \int_V M \, dv. \tag{5}$$

N_f and N_m are functions of the ratio γ of cylinder length to diameter and the susceptibility χ of the material. For ferromagnetic or ferrimagnetic materials, this χ should be regarded as an effective χ, similar to the differential susceptibility dM/dH at the corresponding magnetic state. In [58], the definition of N_m is limited to $\chi = 0$.

III. N_m and N_f for $\chi = 0$ Determined by Inductance Calculations

Brown [29] showed how N_m could be determined using a self-inductance calculation in which a uniformly magnetized cylinder was modeled as a solenoid. In fact, both N_m and N_f may be calculated using the *mutual* inductance of two model solenoids of the same diameter. N_m is obtained when the solenoids have the same length, and the problem reduces to the self-inductance calculation. N_f is obtained when the length of one of the model solenoids approaches 0, and the problem is that of the mutual inductance of a solenoid and a single-turn loop located at its midplane. In this section we calculate exact values of N_m and N_f for $\chi = 0$ and a wide range of γ.

A. Formulas for Inductance

An exact formula for the self-inductance L_s of a thin solenoid of length $2l$, radius a, and number of turns n is [61]

$$L_s = [2\mu_0 n^2/(3l^2)] \{(a^2 + l^2)^{1/2} \cdot [l^2 F(k_s) + (a^2 - l^2)E(k_s)] - a^3\}, \tag{6}$$

where $F(k_s)$ and $E(k_s)$ are the complete elliptic integrals of the first and second kind of modulus k_s, which is defined by

$$k_s^2 = a^2/(a^2 + l^2), \tag{7}$$

and μ_0 is the permeability of vacuum.

An exact formula for the mutual inductance L_m of the same thin solenoid and a coaxial single-turn loop of the same radius at its midplane is [62]

$$L_m = (\mu_0 na/k_m) [F(k_m) - E(k_m)], \tag{8}$$

where the modulus k_m is defined by

$$k_m^2 = 4a^2/(4a^2 + l^2). \tag{9}$$

Cohen [63] derived an exact general formula for the mutual inductance of two concentric coaxial thin solenoids (denoted by subscripts 1 and 2). We have used it successfully for these calculations, as an alternative to (6) and (8), with $a_2 = a_1$, in the limits $l_2 = l_1$ (for N_m) and $l_2 \to 0$ (for N_f).

B. Relationship between N_m and L_s, N_f and L_m

The flux density $\boldsymbol{B}$ in a magnetic material is related to the internal field $\boldsymbol{H}$ and the magnetization $\boldsymbol{M}$: $\boldsymbol{B} = \mu_0(\boldsymbol{H} + \boldsymbol{M})$, where $\boldsymbol{H}$ is, in general, related to the applied and demagnetizing fields as defined for ellipsoids in (1). Thus $\boldsymbol{B} = \mu_0(\boldsymbol{H}_a + \boldsymbol{H}_d + \boldsymbol{M})$. Following Brown [29], we define $\boldsymbol{B}'$ as the Amperian flux density:

$$\boldsymbol{B}' = \boldsymbol{B} - \mu_0 \boldsymbol{H}_a = \mu_0(\boldsymbol{H}_d + \boldsymbol{M}). \tag{10}$$

When $\chi = 0$, a cylinder in an axial field has a uniform magnetization $\boldsymbol{M}$. An ideal thin solenoid carrying current I through n turns over a length $2l$ is equivalent, with respect to the $\boldsymbol{B}'$ field, to a longitudinally magnetized cylinder coincident with it [29]. Thus the cylinder can be modeled as a solenoid with the same $\boldsymbol{M}$, and its average $\boldsymbol{H}_d$ can be obtained from $\boldsymbol{M}$ and average $\boldsymbol{B}'$ using (10). We take the solenoid as having one turn ($n = 1$), so

$$M = I/(2l). \tag{11}$$

For the entire volume, we can obtain the average $\boldsymbol{B}'$ from the average flux Φ in the solenoid as

$$\langle B' \rangle = \Phi/(\pi a^2). \tag{12a}$$

Thus the average demagnetizing field can be obtained from (10) and (12a) as

$$\langle H_d \rangle = \Phi/(\mu_0 \pi a^2) - M. \tag{13a}$$

The definition of self-inductance is

$$L_s = \Phi/I. \tag{14a}$$

From (11), (13a), and (14a), we obtain the final expression for the magnetometric demagnetizing factor:

$$N_m \equiv -\langle H_d \rangle / M = 1 - 2lL_s/(\mu_0 \pi a^2). \tag{15}$$

For N_f, we obtain the average $\boldsymbol{B}'$ at the midplane from the flux Φ_0 in the one-turn secondary loop of radius a:

$$\langle B' \rangle = \Phi_0/(\pi a^2). \tag{12b}$$

The average demagnetizing field is

$$\langle H_d \rangle = \Phi_0/(\mu_0 \pi a^2) - M. \quad (13b)$$

The definition of mutual inductance is

$$L_m = \Phi_0/I. \quad (14b)$$

The final expression for the fluxmetric demagnetizing factor is

$$N_f \equiv -\langle H_d \rangle / M = 1 - 2lL_m/(\mu_0 \pi a^2). \quad (16)$$

Equations (15) and (16) have been derived, by direct integration rather than inductance formulas, by Joseph [35].

C. Results

Values of $N_m(\chi = 0)$ and $N_f(\chi = 0)$ as functions of γ $(= l/a)$ computed using (6), (15), (8), and (16) are given in Table I. For N_m, the data agree with those given by Brown [29], [31]. For N_f, the data agree with those obtained by Joseph [35] and by Chen and Li [38]. In Table I we also give N for ellipsoids of revolution with longitudinal axes $2l$ and transverse axes $2a$ calculated from well-known formulas [4], [59], [60].

IV. One-Dimensional Model for Long Cylinders

A. Calculation of M

Assume that a cylinder of length $2l$ and diameter $2a$ is located in a uniform applied field $\boldsymbol{H}_a$ along the z axis, as shown in Fig. 1. The material has constant susceptibility χ, which leads to

$$\boldsymbol{B} = \mu_0(\boldsymbol{M} + \boldsymbol{H}) = \mu_0 \boldsymbol{M}(1 + 1/\chi) \quad (17)$$

at any point inside the cylinder. Since $\nabla \cdot \boldsymbol{B} = 0$, the volume magnetic pole density, proportional to $\nabla \cdot \boldsymbol{M}$, equals 0 inside the cylinder; that is, all poles are on the surface.

We further assume for this one-dimensional model that M_z, the z component of $\boldsymbol{M}$, is uniform in each cross section of the cylinder, and can be expressed by a scalar quantity as

$$M(z) = M_z(z) = \sum_{i=0}^{n} M_{2i}(z/l)^{2i}, \quad (18)$$

where $M_{2i}(i = 0, 1, \cdots, n)$ are constants. ($\boldsymbol{B}$, $\boldsymbol{H}_a$, and $\boldsymbol{H}_d$ can also be written as scalar quantities.)

For a section of cylinder of length dz at z,

$$\oint \boldsymbol{M} \cdot d\boldsymbol{s} = \pi a^2 dM(z) + 2\pi a M_r(z) dz = 0, \quad (19a)$$

because $\oint \boldsymbol{M} \cdot d\boldsymbol{s} = \int \nabla \cdot \boldsymbol{M}\, dv$ and $\nabla \cdot \boldsymbol{M} = 0$. $M_r(z)$ is the radial component of $\boldsymbol{M}$ at the side surface. Substituting $\sigma(z) = \mu_0 M_r(z)$ gives, on the side surface, the surface magnetic pole density

$$\sigma(z) = -\tfrac{1}{2}\mu_0 a\, dM(z)/dz = -(\mu_0 a/l) \sum_{i=0}^{n} i M_{2i}(z/l)^{2i-1}. \quad (19b)$$

TABLE I
EXACT FLUXMETRIC AND MAGNETOMETRIC DEMAGNETIZING FACTORS N_f AND N_m FOR $\chi = 0$[a]

γ	$N_m(0)$	$N_f(0)$	N
0.00001	0.9999	0.9999	1.0000
0.0001	0.9994	0.9993	0.9998
0.001	0.9950	0.9949	0.9984
0.01	0.9650	0.9638	0.9845
0.02	0.9389	0.9364	0.9694
0.03	0.9161	0.9124	0.9546
0.04	0.8954	0.8905	0.9402
0.05	0.8764	0.8703	0.9262
0.06	0.8586	0.8513	0.9125
0.07	0.8419	0.8333	0.8991
0.08	0.8261	0.8163	0.8860
0.09	0.8110	0.8001	0.8733
0.10	0.7967	0.7845	0.8608
0.12	0.7698	0.7553	0.8367
0.14	0.7450	0.7281	0.8137
0.16	0.7219	0.7027	0.7917
0.18	0.7004	0.6789	0.7706
0.20	0.6802	0.6565	0.7505
0.22	0.6611	0.6352	0.7312
0.24	0.6432	0.6151	0.7126
0.26	0.6262	0.5960	0.6948
0.28	0.6101	0.5778	0.6778
0.30	0.5947	0.5604	0.6614
0.32	0.5801	0.5438	0.6456
0.34	0.5662	0.5279	0.6304
0.36	0.5530	0.5127	0.6158
0.38	0.5403	0.4982	0.6017
0.40	0.5281	0.4842	0.5882
0.45	0.4999	0.4516	0.5563
0.50	0.4745	0.4221	0.5272
0.55	0.4514	0.3952	0.5005
0.60	0.4303	0.3705	0.4758
0.65	0.4110	0.3480	0.4531
0.70	0.3933	0.3273	0.4321
0.75	0.3770	0.3082	0.4126
0.80	0.3619	0.2905	0.3944
0.90	0.3349	0.2592	0.3618
1.0	0.3116	0.2322	0.3333
1.1	0.2911	0.2089	0.3083
1.2	0.2731	0.1886	0.2861
1.3	0.2572	0.1710	0.2664
1.4	0.2429	0.1555	0.2488
1.6	0.2186	0.1298	0.2187
1.8	0.1986	0.1096	0.1941
2.0	0.1819	0.09351	0.1736
2.5	0.1501	0.06544	0.1351
3.0	0.1278	0.04799	0.1087
3.5	0.1112	0.03653	0.08965
4	0.09835	0.02865	0.07541
5	0.07991	0.01889	0.05582
6	0.06728	0.01334	0.04323
7	0.05809	0.009904	0.03461
8	0.05110	0.007635	0.02842
9	0.04562	0.006061	0.02382
10	0.04119	0.004927	0.02029
20	0.02091	0.001245	0.006749
50	0.008438	0.0001999	0.001443
100	0.004232	0.00004999	0.0004299
200	0.002119	0.00001250	0.0001248
500	0.0008483	0.00000200	0.00002363
1000	0.0004243	0.00000050	0.000006601

[a]Factors were calculated as functions of γ using inductance formulas. For comparison, N is the demagnetizing factor for ellipsoids.

On the end planes of the cylinder, we have uniform surface magnetic pole densities:

$$\sigma(\pm l) = \pm \mu_0 M(l) = \pm \mu_0 \sum_{i=0}^{n} M_{2i}. \quad (20)$$

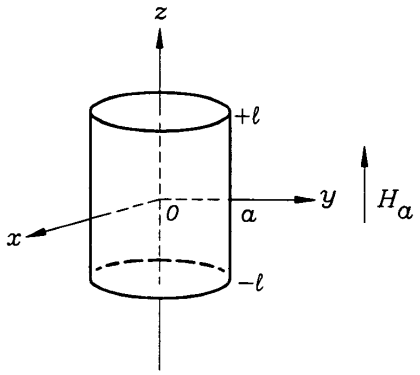

Fig. 1. Cylinder geometry and coordinate system.

Although the side surface magnetic pole density is a function of z only, our assumptions of both uniform M_z and uniform $\sigma(\pm l)$ are, in fact, contradictory for constant χ; a uniform $\sigma(\pm l)$ and the side pole density would produce a nonuniform H_{dz}, the z component of the demagnetizing field, which would lead to a nonuniform M_z. However, if γ ($= l/a$) is large (≥ 10), and if we consider only N_f, for which the middle part of the cylinder is more important, this one-dimensional model is a good approximation.

B. Calculation of N_f and N_m for Long Cylinders ($\gamma \geq 10$)

In this model, in a given H_a, the demagnetizing field H_d is a function of z:

$$H_d(z) = H_{d1}(z) + H_{d2}(z), \tag{21}$$

where H_{d1} and H_{d2} are the demagnetizing fields produced by the side poles and the end poles, respectively.

At a point $z = \zeta$ on the z axis,

$$H_{d1}(\zeta) = -a(2\mu_0)^{-1} \int_{-l}^{+l} \sigma(z)(z - \zeta) \cdot [(z - \zeta)^2 + a^2]^{-3/2}\, dz = \sum_{i=0}^{n} F_{1i}(\zeta) M_{2i}, \tag{22a}$$

where

$$F_{1i}(\zeta) = ia^2(2l^{2i})^{-1} \int_{-l}^{+l} z^{2i-1}(z - \zeta) \cdot [(z - \zeta)^2 + a^2]^{-3/2}\, dz. \tag{22b}$$

The fields produced by the end poles at $z = \pm l$ are

$$H_{d2\pm}(\zeta) = -(2\mu_0)^{-1} \int_0^a \sigma(\pm l)\,(\pm l - \zeta) \cdot r[(\pm l - \zeta)^2 + r^2]^{-3/2}\, dr = \tfrac{1}{2} M(l)\{(l \mp \zeta)[(l \mp \zeta)^2 + a^2]^{-1/2} - 1\}, \tag{23}$$

from which

$$H_{d2}(\zeta) = H_{d2+}(\zeta) + H_{d2-}(\zeta) = \sum_{i=0}^{n} F_2(\zeta) M_{2i}, \tag{24a}$$

where

$$F_2(\zeta) = \tfrac{1}{2}(l + \zeta)[(l + \zeta)^2 + a^2]^{-1/2} + \tfrac{1}{2}(l - \zeta)[(l - \zeta)^2 + a^2]^{-1/2} - 1. \tag{24b}$$

From (3), and considering the z dependence of H and H_d, we have

$$H_d(z) - M(z)/\chi = -H_a. \tag{25}$$

Rewriting the variable ζ in H_{d1}, F_{1i}, H_{d2}, and F_2 as z, and substituting (22a) and (24a) into (21), and (18) and (21) into (25), we obtain

$$\sum_{i=0}^{n} [F_{1i}(z) + F_2(z) - (z/l)^{2i}/\chi] M_{2i} = -H_a. \tag{26}$$

This is a general equation relating the expansion coefficients M_{2i} of magnetization, the applied field H_a, the susceptibility χ, and the position z for a cylinder of length $2l$ and diameter $2a$. In our problem, H_a, l, a, and χ are given, and the $n + 1$ coefficients M_{2i} are unknown. We can choose $n + 1$ positions, $z = z_0, z_1, \cdots, z_n$, and get a set of $n + 1$ linear equations. M_{2i} ($i = 0, 1, \cdots, n$) are then obtained by solving these equations simultaneously. N_f and N_m can be obtained according to (4), (5), and (25) as

$$N_f = -H_d(0)/M_0 = H_a/M_0 - 1/\chi, \tag{27}$$

$$N_m = -\langle H_d \rangle / \langle M \rangle = H_a/\langle M \rangle - 1/\chi, \tag{28}$$

where the $\langle\ \rangle$ brackets denote the volume average, and

$$\langle M \rangle = l^{-1} \int_0^l M(z)\, dz = \sum_{i=0}^{n} M_{2i}/(2i + 1). \tag{29}$$

In principle, the larger the number of terms in the expansion equation (26), the more accurate are the results. However, if n is too large, the computed function $M(z)$ oscillates. For computation, $n = 12$ is a practical choice, and

$$z_i = il/12, \quad (i = 0, 1, \cdots, 12), \tag{30}$$

$$H_a = 1, \tag{31a}$$

$$a = 1 \tag{31b}$$

Table II and Fig. 2(a) and 2(b) give the calculated N_f as functions of γ and χ for $-1 \leq \chi \leq 10^9$. When $\chi \to \infty$, $\boldsymbol{H}_d$ is uniform in the cylinder ($\boldsymbol{H}_d = -\boldsymbol{H}_a$), and $\boldsymbol{M}$ close to the ends is very small. As a result, values of $N_m(\chi \to \infty)$ obtained from this model are expected to be fairly accurate due to rather small end effects. Similar data were presented in [64]. Fig. 3 gives N_m and N_f as functions of γ when $\chi = 0.001$ and 10^9. The demagnetizing factors N for ellipsoids (dashed curve) are located between N_m and N_f for $\chi \to \infty$.

TABLE II
N_f AS FUNCTION OF γ AND χ CALCULATED USING THE ONE-DIMENSIONAL MODEL[a]

γ	10	20	50	100	200	500	1000	2000
χ	(10^{-3})	(10^{-3})	(10^{-4})	(10^{-5})	N_f (10^{-5})	(10^{-6})	(10^{-7})	(10^{-7})
−1	3.965	1.130	1.900	4.776	1.196	1.917	4.796	1.199
−0.8	4.239	1.162	1.931	4.852	1.215	1.945	4.865	1.216
−0.4	4.642	1.210	1.972	4.944	1.237	1.980	4.950	1.237
0	4.963	1.248	1.999	5.000	1.250	2.000	5.000	1.250
0.1	5.037	1.256	2.005	5.011	1.252	2.004	5.010	1.252
0.2	5.108	1.265	2.011	5.021	1.255	2.007	5.018	1.255
0.5	5.315	1.289	2.026	5.047	1.260	2.016	5.040	1.260
1	5.639	1.328	2.049	5.082	1.268	2.027	5.067	1.267
2	6.231	1.401	2.089	5.135	1.277	2.040	5.100	1.275
5	7.695	1.616	2.191	5.247	1.293	2.058	5.143	1.286
10	9.377	1.967	2.352	5.394	1.308	2.071	5.168	1.292
20	11.23	2.565	2.688	5.664	1.332	2.083	5.187	1.296
50	13.21	3.600	3.803	6.494	1.395	2.106	5.211	1.299
100	14.14	4.294	5.448	8.132	1.500	2.141	5.238	1.302
200	14.68	4.776	7.497	11.77	1.734	2.210	5.288	1.305
500	15.03	5.126	9.800	19.91	2.661	2.414	5.438	1.316
10^3	15.15	5.255	10.90	26.32	4.221	2.808	5.684	1.333
2×10^3	15.21	5.322	11.53	31.12	6.275	3.889	6.186	1.369
5×10^3	15.25	5.363	11.95	34.78	8.642	7.570	8.223	1.474
10^4	15.26	5.377	12.09	36.16	9.779	11.68	13.12	1.669
2×10^4	15.27	5.384	12.16	36.88	10.44	15.47	22.71	2.237
5×10^4	15.27	5.388	12.21	37.33	10.87	18.77	38.36	4.620
10^5	15.27	5.390	12.22	37.48	11.02	20.11	47.73	7.811
2×10^5	15.28	5.390	12.23	37.55	11.10	20.83	53.77	11.10
5×10^5	15.28	5.391	12.23	37.60	11.14	21.28	57.94	14.19
10^6	15.28	5.391	12.24	37.62	11.16	21.44	59.43	15.50
10^7	15.28	5.391	12.24	37.63	11.17	21.58	60.82	16.83
10^9	15.28	5.391	12.24	37.63	11.17	21.59	60.98	16.99
∞	15.30		12.11	37.20				

[a]The row for $\chi = 0$ is comparable to data for $N_f(0)$ in Table I. The last row gives $N_f(\infty)$ calculated by Templeton and Arrott [45].

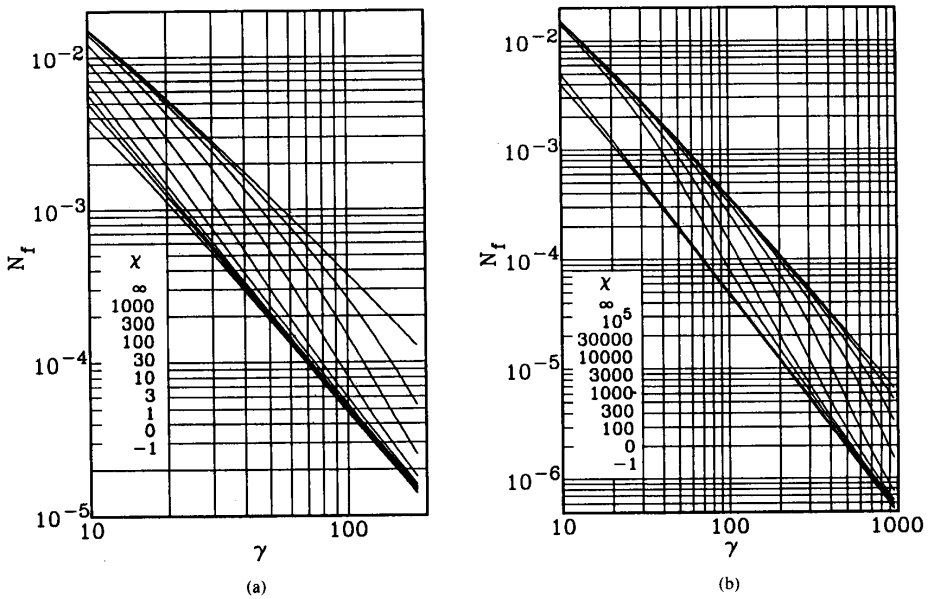

Fig. 2. Calculated N_f from the one-dimensional model. (a) For $10 \leq \gamma < 200$, the curves from top to bottom are for $\chi = \infty$, 1000, 300, 100, 30, 10, 3, 1, 0, and −1. (b) For $10 \leq \gamma < 1000$, the curves from top to bottom are for $\chi = \infty$, 10^5, 3×10^4, 10^4, 3×10^3, 10^3, 300, 100, 0, and −1.

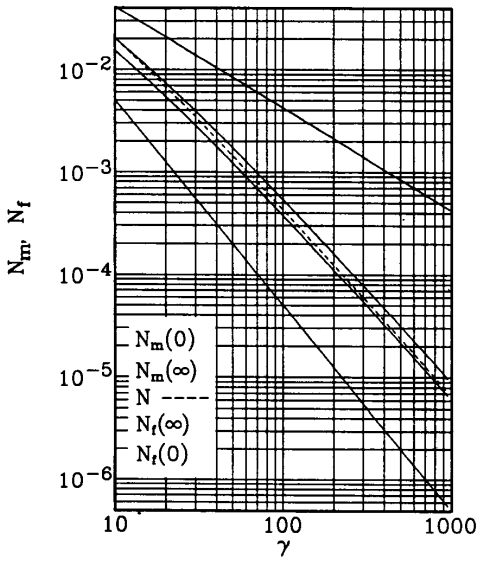

Fig. 3. N_m and N_f for $10 \leq \gamma < 1000$. The solid curves from top to bottom are $N_m(\chi = 0)$, $N_m(\chi \to \infty)$, $N_f(\chi \to \infty)$, and $N_f(\chi = 0)$. The dashed curve is N for ellipsoids.

Earlier results for $\gamma > 10$ exist for N_f but not for N_m. Würschmidt's result for $\gamma = 50$ and $\chi \to \infty$ is 3.4% smaller than our result [20], [21]. Neumann and Warmuth's results deviate from our results by 1.5%, 0.0%, −3.4%, −5.3%, and −8.6% for $\gamma = 10$, 20, 50, 100, and 1000 [22]. For $\chi \to \infty$, the maximum deviation of the results of Stäblein and Schlechtweg from our results is 3%; but for their smallest χ (12.56), the maximum difference is above 30% [23]. Templeton and Arrott's [45] results for $\chi \to \infty$ (Table II) are the most accurate, and our data agree within 1.1%. Compared with the exact results for $\chi = 0$ in Table I, the data in Table II have errors of 0.7%, 0.2%, and 0.0% for $\gamma = 10$, 20, and $\gamma \geq 50$.

V. Two-Dimensional Model for Short Cylinders

A. Calculation of Surface Pole Density

The magnetization, in general, varies throughout the cylinder in both the radial and axial directions. A calculation of demagnetizing factors for a short cylinder ($\gamma < 10$) must take this variation into account, especially near the corners, where the magnetization sharply diverges for susceptibilities far from 0. As in the one-dimensional model, we assume that the cylinder consists of material with constant χ, so the demagnetizing fields are completely specified by the surface pole density.

To obtain the distribution of poles on the surface for a specified susceptibility, we divide the surface of the cylinder into a set of nonoverlapping elements of uniform pole density. With the cylindrical symmetry there is no azimuthal dependence of the pole distribution, and we are therefore able to use elements in the shape of rings about the central axis. We solve the set of equations that describes the interaction between these rings of surface poles and use the resulting distribution to obtain the magnetometric and fluxmetric demagnetizing factors.

The method of dividing the surface of a magnetized body into a set of interacting elements of uniform pole density has been used before for the calculation of the magnetic fields of rectangular bodies. Ruehli and Ellis [65] assumed a constant susceptibility, and Normann and Mende [66] used a field dependent magnetization with the assumption that the volume pole distribution is negligible. Both of these studies were interested primarily in the field and magnetization distributions rather than the demagnetizing factors. A method that involves dividing the volume into uniformly magnetized elements was used by Brug and Wolf [57] for the case of thin disks that undergo magnetic phase transitions. They used a demagnetizing matrix that was derived by Hegedus, Kadar, and Della Torre [67], [68] for interacting volume elements in cylindrical geometries. Volume elements have also been used by Soinski [69] for rectangular and ring-shaped samples. A method of obtaining demagnetizing fields in bodies of arbitrary shape was presented by Vallabh Sharma [36] using rectangular volume elements. Templeton and Arrott [45] used the principle that the magnetic potential is 0 at each point on a grid inside a body with infinite susceptibility. They calculated the demagnetizing factors of cylinders and bars and later extended this to the case of a material that saturates [70].

The following method solves for the pole distribution at the surface of a cylinder for an arbitrary value of the susceptibility. The surface is divided into rings of area $\pi(r_2^2 - r_1^2)$ on the end planes of the cylinder and into rings of area $2\pi a(z_2 - z_1)$ on the side surface of the cylinder. The cylinder diameter is $2a$, r_1 and r_2 are the inner and outer radii of the end-surface ring, and z_1 and z_2 are the side-surface ring limits. The z and r components of the demagnetizing field at a point i that results from the surface poles σ_j at each ring are given by

$$H_{dz}^i = -\sum_j N_z^{ij}\,\sigma_j/\mu_o, \tag{32a}$$

$$H_{dr}^i = -\sum_j N_r^{ij}\,\sigma_j/\mu_o, \tag{32b}$$

where, for example, N_r^{ij} is a scalar factor that relates the surface pole on the jth ring to the r component of the demagnetizing field that it produces at the ith ring. A method of calculating these factors is given in the Appendix.

The interactions between the surface poles at each ring is specified using the equation $\boldsymbol{M} = \chi(\boldsymbol{H}_a + \boldsymbol{H}_d)$. The demagnetizing field $\boldsymbol{H}_d$, given in (32), is written in terms of the magnetization at each ring using $\sigma_j/\mu_0 = \boldsymbol{n} \cdot \boldsymbol{M}^j \equiv \boldsymbol{M}_n^j$, where $\boldsymbol{n}$ is the unit vector outward normal to the surface of the ring, and $\boldsymbol{M}^j$ is the magnetization at the jth ring. The resulting equations are for the magnetization at each point,

$$M_z^i = \chi\left(H_a - \sum_j N_z^{ij} M_n^j\right), \tag{33a}$$

$$M_r^i = -\chi \sum_j N_r^{ij} M_n^j, \tag{33b}$$

TABLE III
N_f VALUES CALCULATED BY SURFACE AND VOLUME METHODS (N_{fs} AND N_{fv}) USING 74 SIDE RINGS

χ	−1		0.0001		10000	
γ	N_{fs}	N_{fv}	N_{fs}	N_{fv}	N_{fs}	N_{fv}
0.1	0.82568	0.82582	0.78460	0.78461	0.73312	0.064998
1	0.23196	0.23195	0.23258	0.23225	0.22912	0.015670
10	0.018951	0.0042004	0.0081227	0.0049267	0.016904	0.00099941

where we have constrained the applied field to be in the axial direction. Because only the normal component of M is needed at each point, the equations can be rewritten as

$$H_a = \chi^{-1} M_n^i + \sum_j N_z^{ij} M_n^j \quad \text{(rings on the top end-plane)}, \tag{34a}$$

$$H_a = -\chi^{-1} M_n^i + \sum_j N_z^{ij} M_n^j \quad \text{(rings on the bottom end-plane)}, \tag{34b}$$

$$0 = \chi^{-1} M_n^i + \sum_j N_r^{ij} M_n^j \quad \text{(rings on the side surface)}. \tag{34c}$$

With the surface of the cylinder divided into n rings, there will be a set of n simultaneous linear equations. These equations are solved for M_n at each ring using matrix inversion [71].

The number of rings required to adequately specify the surface pole density depends on how rapidly the pole distribution varies. For both large susceptibilities and susceptibilities near -1, the pole distribution diverges sharply near the corner of the cylinder. To reduce the total number of rings, the density of the rings is made roughly proportional to the pole density. For the case of infinite susceptibility, the pole density near the corner at the end-plane is approximated as [45]

$$\sigma_0(r, \pm l) \propto \pm[(1 - r/a)^{-1/3} - (1 + r/a)^{-1/3}]. \tag{35}$$

We let the width of the rings Δr be inversely proportional to σ_0 near the corner of the cylinder, which gives

$$\Delta r = \{a_0 + a_1[(1 - r/a)^{-1/3} - (1 + r/a)^{-1/3}]\}^{-1}. \tag{36}$$

A similar equation determines the width of the rings on the side surface of the cylinder. The adjustable parameters a_0 and a_1 are determined by the total number of rings used in the calculation. A total of 148 rings was used, 37 on each end-plane and 74 on the side of the cylinder. For $\gamma = 10$, 20, and 50, the calculations were repeated with 8 end-plane rings and 132 side rings.

B. Calculation of N_m and N_f

After obtaining the surface pole distribution, there are two ways to calculate the demagnetizing factors, based on the two equations

$$N_{f,m} = -\langle H_d \rangle / \langle M_z \rangle = H_a / \langle M_z \rangle - \chi^{-1}, \tag{37a}$$

$$N_{f,m} = -\langle H_d \rangle / \langle M_z \rangle = -\langle H_d \rangle / [\chi(H_a + \langle H_d \rangle)], \tag{37b}$$

where H_d and M_z are averaged over the midplane for N_f and over the volume for N_m.

For the first method, using (37a), $N_{f,m}$ is calculated from $\langle M_z \rangle$. We have $\oint \boldsymbol{M} \cdot d\boldsymbol{s} = 0$ for a material with constant susceptibility. Therefore, for each transverse cross section of the cylinder, the average M_z multiplied by the cross-sectional area S equals the surface integration of M_n over the cylinder surface above the cross section. In the case of N_f, the cross section is taken to be the midplane. We have, from (37a),

$$N_f = H_a S \Big/ \int_{S_1} M_n \, ds - \chi^{-1} = H_a S \Big/ \sum_j M_n^j s_j - \chi^{-1} \tag{38}$$

where S_1 is the surface consisting of the top half of the cylinder, s_j is the area of the jth ring, and the sum is over the rings on the top end-plane and on the side surface above the midplane. To calculate N_m, a series of cross sections corresponding to each side-surface ring is considered, and the volume-averaged M_z is calculated from a weighted average over these cross sections.

The second method, using (37b), requires a calculation of $\langle H_d \rangle$. We use (32a), with i denoting an interior point of the cylinder. Again, the average is taken over the midplane for N_f and over the volume for N_m.

Since the first method involves surface flux calculations, while the second involves interior field calculations, we refer to them as the surface and the volume methods, respectively. Table III gives some examples of the results obtained from both methods. We see from this table that the results do not agree, especially for large γ or large χ. The differences are even larger for N_m. The source of the disagreement is a systematic error that is due almost entirely to the finite number of elements with which the surface pole density is calculated.

The field produced by a magnetic pole is very sensitive to the distance r between the pole and the point at which the field is considered, with an r^{-2} dependence. In the two-dimensional model, the division of the surface of the cylinder into rings will produce a discretization error because H_d is calculated in the center of a region of uniform pole density. This error is mainly due to the division of the side surface; at the center of each ring on this surface, the normal component of H_d is produced by poles on the ring itself with significant contribution from poles on adjacent rings. For the end planes, the poles on the same

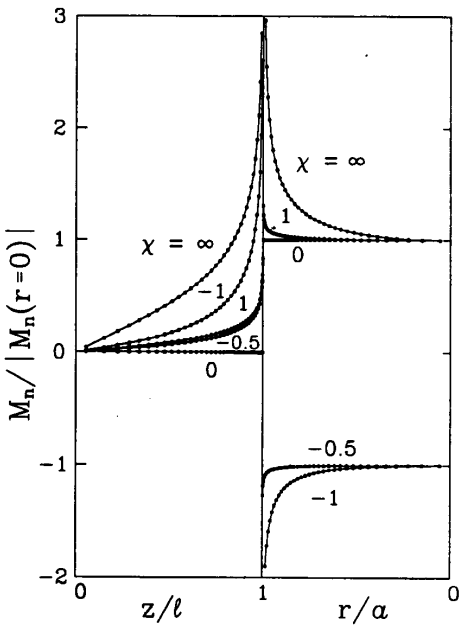

Fig. 4. Variation of normalized M_n on the surface of a cylinder with $\gamma = 1$ for selected values of susceptibility. On the left half of the figure, corresponding to the cylinder side, the curves from top to bottom are for $\chi = \infty$, -1, 1, -0.5, and 0. On the right half, corresponding to the cylinder end, the curves are for $\chi = \infty$, 1, 0, -0.5, and -1.

surface do not contribute to the normal component of H_d, except for the pole at the point being considered. A region of uniform pole density adjacent to the point does not produce a discretization error.

Fig. 4 gives the surface pole distribution of a cylinder with $\gamma = 1$ for $\chi = -1$, -0.5, 0.0001, 1, and 10 000, calculated with the two-dimensional model. The normalized pole density is expressed as $M_n/|M_n(r=0)|$. Therefore, all the curves have the actual sign of the pole density when H_a is positive. The curves shown are for the top half of the cylinder with $z > 0$; they are odd functions of z. As can be seen from the figure, when $\chi \to \infty$, the side poles are broadly distributed with a larger density, and this should give a relatively large error. The side poles are narrowly distributed for $\chi < 0$, giving a small error. For the cases of small or zero side-pole density (low or zero χ), the error will be small or zero. The error becomes larger as γ increases because the size of the rings on the side surface also increases. The relative effect of the end poles increases and the error decreases as γ decreases.

This systematic error is correctable if it is not too large. For the surface and volume methods, we write the demagnetizing factors as N_s and N_v, and write $\langle M_z \rangle$ and $\langle H_d \rangle$ as M_{zs} and H_{dv}, respectively. For simplicity, the corrected quantities are written as N, M_z, and H_d. H_a is arbitrarily set equal to 1. From (37), we have

$$N_s = M_{zs}^{-1} - \chi^{-1}, \tag{39a}$$

$$N = M_z^{-1} - \chi^{-1}, \tag{39b}$$

$$N_v^{-1} = -\chi(H_{dv}^{-1} + 1), \tag{39c}$$

$$N^{-1} = -\chi(H_d^{-1} + 1). \tag{39d}$$

We assume that the error in the surface pole density calculation is not too large so that

$$H_{dv}/H_d \simeq M_{zs}/M_z. \tag{39e}$$

Thus we have from (39)

$$N_v(1 + N\chi)/[N(1 + N_v\chi)] = (1 + N\chi)/(1 + N_s\chi). \tag{40a}$$

Solving (40a) for N gives the interpolation/extrapolation equation

$$N = N_v(1 + N_s\chi)/(1 + N_v\chi). \tag{40b}$$

We use (40b) and the results (up to 5 significant digits) from the two methods to obtain the final N_f and N_m. They are presented in Tables IV and V and Figs. 5, 6, and 7. The entries in Table III provide data for illustrative computations. Values for $\gamma \leq 10$ were obtained with the 74-side-ring calculation. The values for $\gamma = 20$ and 50 are from the 132-side-ring calculation, which gives a smaller discretization error for these cases. As an example of the worst case, N_f for $\chi = 10\,000$ and $\gamma = 20$ is 55.46×10^{-4} when computed with 74 side rings, compared to 53.85×10^{-4} for 132 side rings.

With the corrected $N_{f,m}$ we can correct M_z and H_d using (39b) and (39d) and compare them with M_{zs} and H_{dv} calculated from (39a) and (39c). We find that, for all N_f and N_m, the discretization error is less than 10%, giving a demagnetizing factor error of $< 1\%$. Exceptions are when $\gamma = 20$ and $\chi \geq 100$ for the 74-side-ring calculation, and when $\gamma = 50$ and $\chi \geq 100$ or $\gamma = 10$ and $\chi = 10\,000$ for the 132-side-ring calculation. Thus (39e) is rather accurate in most cases and the interpolation/extrapolation approach is valid.

A comparison can be made with less-general published results obtained for specific values of χ. The results agree with the exact self-inductance calculations in Table I to four significant figures except for N_m for $\gamma > 1$ when, in the worst case, the error is 0.12%. The two-dimensional calculation for N_m can be compared with N_m data deduced from the work of Taylor [40], [41] as shown in Section VI-A. From Taylor's data, we calculate five values each of $N_m(-1)$ and $N_m(\infty)$ for $0.25 \leq \gamma \leq 4$ (Table VI). The greatest difference between the two-dimensional results and Taylor's method is 0.22% for $N_m(-1)$ and 0.17% for $N_m(\infty)$. For $N_f(\infty)$, the results are compared with the values calculated by Templeton and Arrott [45]. The largest deviation is 0.98% at $\gamma = 10$.

The results of N_f for $\gamma \geq 10$ can be compared with our one-dimensional calculation (Table II). The deviations of the one-dimensional from the two-dimensional results are -1.2%, -1.2%, 0.6%, 1.8%, 0.7%, and -4.2% for $\gamma = 10$ and $\chi = 10\,000$, 100, 10, 1, 0, and -1, respectively. For $\gamma = 20$ and 50 the maximum deviation reduces to 1.2% and 1.9%, respectively. Such deviations are due mainly to the approximations made in the one-dimensional model.

TABLE IV
N_f AS FUNCTION OF χ AND γ CALCULATED USING THE TWO-DIMENSIONAL MODEL

χ	−1	−0.9	−0.7	−0.5	−0.3	0.0001	0.3	1	3	10	100	10000
γ	$N_f(10^{-4})$											
0.01	9781	9728	9690	9669	9655	9639	9628	9610	9586	9562	9548	9544
0.02	9576	9513	9453	9418	9393	9365	9345	9313	9268	9225	9195	9191
0.03	9383	9316	9242	9196	9163	9125	9097	9052	8990	8929	8888	8881
0.04	9201	9132	9048	8993	8952	8906	8872	8817	8739	8663	8612	8603
0.05	9028	8957	8865	8803	8756	8704	8664	8599	8508	8419	8359	8349
0.07	8704	8631	8528	8454	8398	8334	8285	8206	8094	7984	7909	7879
0.1	8265	8188	8073	7988	7922	7846	7788	7693	7558	7425	7335	7321
0.2	7060	6974	6840	6738	6659	6566	6494	6378	6214	6054	5945	5929
0.3	6106	6016	5879	5776	5697	5605	5535	5421	5262	5109	5006	4990
0.4	5309	5223	5093	4999	4926	4843	4780	4679	4539	4405	4316	4302
0.5	4626	4549	4436	4353	4292	4222	4169	4084	3968	3858	3784	3773
0.7	3513	3466	3399	3351	3314	3273	3242	3193	3125	3060	3016	3009
1	2319	2323	2325	2325	2325	2322	2320	2315	2304	2291	2280	2278
1.5	1199	1246	1311	1354	1385	1418	1442	1477	1520	1556	1578	1581
2	689.6	738.4	808.3	857.3	894.0	935.2	965.6	1013	1078	1138	1177	1182
2.5	449.7	487.1	543.0	584.3	616.7	654.4	683.5	731.6	801.5	871.4	920.8	927.7
3	323.7	350.0	391.1	422.8	448.6	479.9	505.0	548.4	616.1	689.2	745.0	752.6
4	199.1	212.3	233.8	251.5	266.8	286.5	303.4	334.8	390.6	461.1	522.5	531.6
5	137.6	144.9	157.0	165.4	176.6	188.9	199.9	221.8	264.8	327.6	390.1	400.1
7	77.75	80.68	85.57	89.81	93.67	99.05	104.1	114.8	139.4	185.1	244.2	255.2
10	41.38	42.47	44.28	45.84	47.27	49.27	51.17	55.41	66.43	93.25	143.1	154.5
20	11.44	11.59	11.83	12.03	12.21	12.45	12.69	13.20	14.61	19.51	42.96	53.85
50	1.937	1.946	1.961	1.974	1.984	1.999	2.012	2.039	2.110	2.337		

TABLE V
N_m AS FUNCTION OF χ AND γ CALCULATED USING THE TWO-DIMENSIONAL MODEL

χ	−1	−0.9	−0.7	−0.5	−0.3	0.0001	0.3	1	3	10	100	10000
γ	$N_m(10^{-4})$											
0.01	9780	9730	9695	9677	9665	9651	9642	9628	9608	9589	9577	9574
0.02	9576	9517	9464	9434	9413	9390	9373	9347	9310	9275	9251	9247
0.03	9385	9323	9259	9220	9192	9162	9139	9103	9052	9000	8967	8960
0.04	9205	9143	9071	9026	8993	8955	8927	8882	8819	8754	8711	8703
0.05	9035	8974	8896	8845	8808	8765	8733	8680	8605	8529	8478	8469
0.07	8721	8660	8575	8516	8471	8420	8380	8315	8221	8127	8062	8050
0.1	8300	8240	8149	8082	8029	7968	7920	7841	7726	7609	7529	7515
0.2	7200	7135	7029	6947	6881	6803	6741	6637	6485	6332	6224	6207
0.3	6393	6318	6200	6108	6035	5948	5880	5768	5604	5440	5327	5306
0.4	5766	5681	5550	5451	5373	5282	5211	5096	4930	4768	4657	4640
0.5	5260	5167	5025	4921	4839	4745	4674	4558	4395	4239	4134	4118
0.7	4488	4382	4226	4114	4029	3933	3862	3749	3596	3455	3363	3349
1	3692	3576	3410	3295	3210	3116	3047	2942	2804	2682	2604	2593
1.5	2860	2744	2580	2469	2388	2301	2238	2144	2023	1921	1858	1850
2	2339	2229	2076	1973	1898	1818	1761	1675	1567	1475	1418	1411
2.5	1979	1878	1737	1643	1574	1501	1449	1370	1270	1184	1131	1124
3	1717	1623	1494	1407	1345	1277	1229	1156	1063	981.8	930.2	922.7
4	1358	1277	1167	1094	1040	983.1	941.8	897.0	796.8	721.7	671.0	663.5
5	1123	1053	958.0	894.5	848.4	798.6	762.7	707.7	634.1	564.1	513.5	505.8
7	834.0	779.6	705.2	655.6	619.5	580.4	552.1	508.2	447.9	386.4	336.2	328.0
10	601.5	560.7	505.1	468.0	440.9	411.5	390.1	356.6	309.6	258.5	210.2	201.3
20	316.8	293.7	262.3	241.6	226.6	210.2	198.3	179.5	152.5	120.9	82.60	72.91
50	128.4	119.1	106.4	97.78	91.53	84.70	79.70	71.77	60.18	46.05		

VI. DISCUSSION

A. $N_{f,m}$ for $\chi = 0, \infty$, and -1

In ellipsoids, a uniform applied field produces a magnetization and a demagnetizing field that are both uniform. In cylinders, the magnetization and the demagnetizing field are both nonuniform except in two cases. For $\chi = 0$, the magnetization is uniform but the demagnetizing field is not. For $\chi \to \infty$, the demagnetizing field is uniform (and exactly opposite to the applied field) but the magnetization is not. For $\chi = -1$, the nonuniform magnetization and nonuniform demagnetizing field in the cylinder combine to exactly cancel the applied field so that the flux density $B = 0$. In these three cases, demagnetizing factors can be calculated more accurately by introducing electromagnetic scalar potentials. Moreover, there are some simple relations among N_{mx}, N_{my}, and N_{mz}, the magnetometric demagnetizing factors along the three principal orthogonal axes.

For $\chi = 0$, a cylinder has N_{mx}, N_{my}, and N_{mz} that are

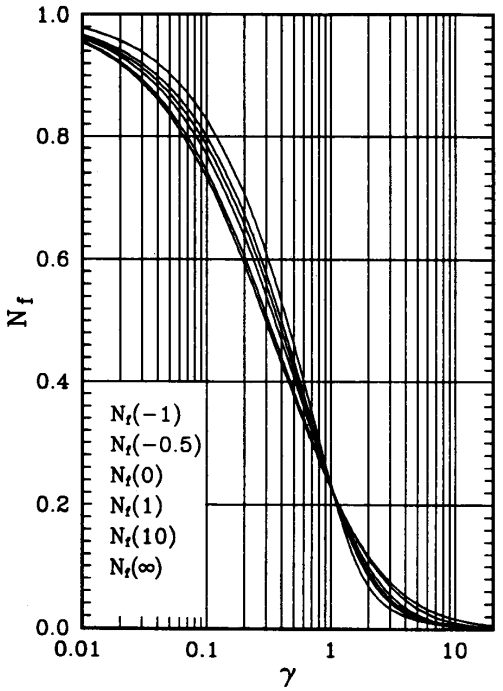

Fig. 5. N_f for $0.01 \leq \gamma \leq 20$ and $-1 \leq \chi < \infty$ from the two-dimensional model, based on Table IV. The curves are for $\chi = -1$, -0.5, 0, 1, 10, and ∞. The curve labels refer to the left side of the figure.

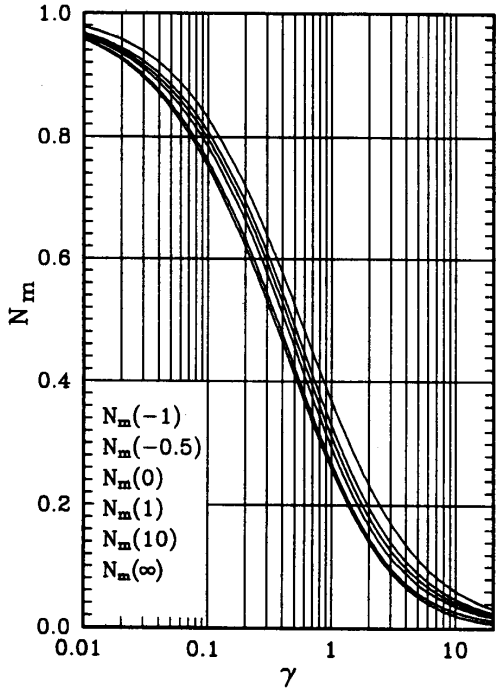

Fig. 6. N_m for $0.01 \leq \gamma \leq 20$ and $-1 \leq \chi < \infty$ from the two-dimensional model, based on Table V. The curves from top to bottom are for $\chi = -1$, -0.5, 0, 1, 10, and ∞.

equivalent to those of a possible ellipsoid of revolution, with

$$N_{mx} + N_{my} + N_{mz} = 1, \tag{41}$$

according to the more general theorem of Brown and Morrish [72]–[74]. As examples from Table I, cylinders with $\gamma = 0.22$, 0.80, and 1.6 are equivalent to ellipsoids with $\gamma = 0.30$, 0.90, and 1.6. A cylinder with $\gamma = 0.9065$ is equivalent to a sphere ($N = 0.3333$) [36]. A cube is also equivalent to a sphere according to the theorem [75]–[77]. Experimentally, for weakly magnetic and saturated ferromagnetic materials, these two shape-isotropic geometries can be used as alternatives to spheres. However, the theorem of Brown and Morrish on the equivalence of a body of arbitrary geometry (including a cylinder) and a possible ellipsoid cannot lead to an *a priori* estimate of the value of $N_m(\chi = 0)$ except for a body with center symmetry, such as a cube.

For cylinders, the transverse magnetometric demagnetizing factors are

$$N_{mx} = N_{my} = \tfrac{1}{2}(1 - N_{mz}). \tag{42}$$

Equations (41) and (42) are valid for N_m only when $\chi = 0$. For $\chi > 0$, the sum is less than 1, while for $\chi < 0$, it is greater than 1. If N_f is considered, rather than N_m, the sum is always less than 1.

For a given γ, values of $N_f(\chi \to \infty)$ and $N_m(\chi \to \infty)$ are rather close to N for ellipsoids. We can fit the $N_f(\infty)$ and $N_m(\infty)$ versus γ data in Table II and Figs. 2 and 3 by simple equations:

$$N_f(\chi \to \infty, \gamma) = N(\gamma)[1 + 0.12(\log \gamma - 3)], \tag{43a}$$

$$N_m(\chi \to \infty, \gamma) = N(\gamma)[1 + 0.25(\log \gamma - 1)], \tag{43b}$$

where the demagnetizing factor $N(\gamma)$ for ellipsoids can be found in Table I. In the range $10 \leq \gamma \leq 100$, (43a) and (43b) fit the model results with maximum deviations of 1% and 1.5%, respectively. Including the results for $\gamma < 10$ in Tables IV and V, the lower boundaries of the γ range with the same indicated errors extend to 2 and 7 for N_f and N_m, respectively.

Taylor calculated the anisotropic electric (α) and magnetic (β) polarizabilities of conducting cylinders [40], [41]. In Taylor's terminology, "conducting" means "without field penetration," so electrically $E = 0$ and magnetically $B = 0$. Therefore we can relate the longitudinal α_{ll} and transverse α_{tt} electric polarizabilities to $N_m(\infty)$, and the longitudinal β_{ll} and transverse β_{tt} magnetic polarizabilities to $N_m(-1)$. For a conducting solid of revolution with volume V_0,

$$\alpha_{ll}/(\epsilon_0 V_0) = N_{mz}(\infty)^{-1}, \tag{44a}$$

$$\alpha_{tt}/(\epsilon_0 V_0) = N_{mx}(\infty)^{-1}, \tag{44b}$$

$$\mu_0 \beta_{ll}/V_0 = [N_{mz}(-1) - 1]^{-1}, \tag{44c}$$

$$\mu_0 \beta_{tt}/V_0 = [N_{mx}(-1) - 1]^{-1}, \tag{44d}$$

where ϵ_0 is the permittivity of vacuum. Equations (44a) and (44b) are in accordance with the analogy between

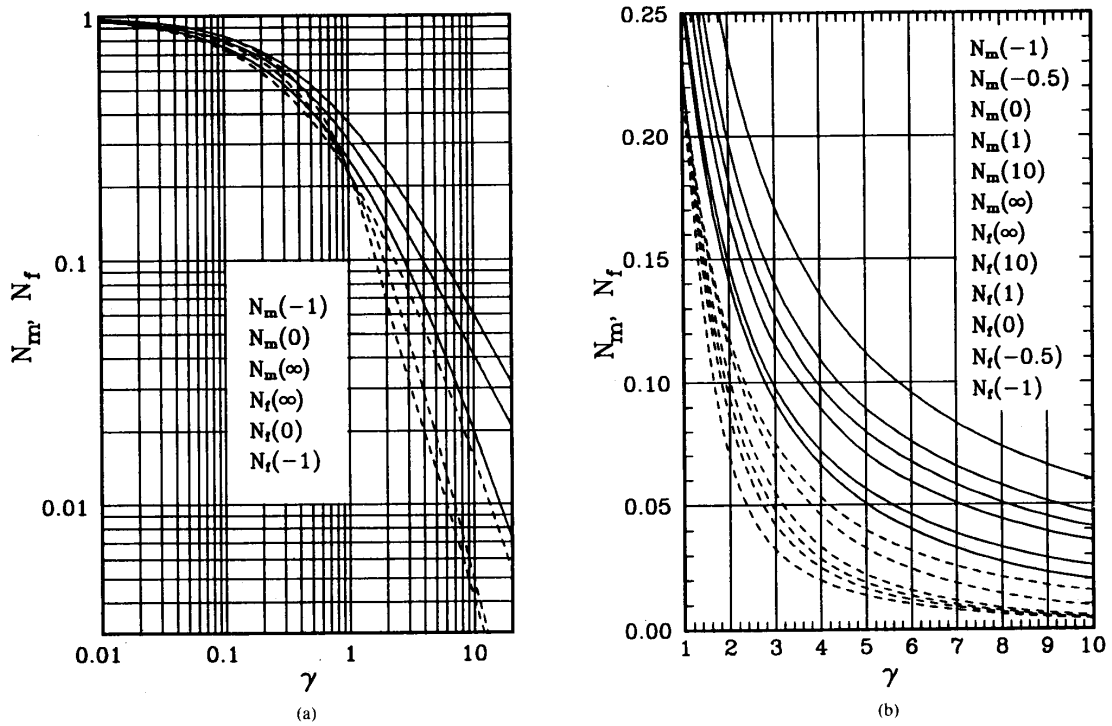

Fig. 7. N_m (solid curves) and N_f (dashed curves) from the two-dimensional model. (a) Logarithmic scale, $0.01 \le \gamma \le 20$. The curve labels refer to the right side of the figure. (b) Linear scale, $1 \le \gamma \le 10$.

TABLE VI
$N_{mz}(\infty)$, $N_{mx}(\infty)$, $N_{mz}(-1)$, and $N_{mx}(-1)$ FOR SHORT CYLINDERS[a]

γ	$N_{mz}(\infty)$	$N_{mx}(\infty)$	$\Sigma(\infty)$	$N_{mz}(-1)$	$N_{mx}(-1)$	$\Sigma(-1)$
0	1	0	1	1	0	1
0.25	0.5712	0.1618	0.8948	0.6764	0.2136	1.1036
0.5	0.4111	0.2371	0.8853	0.5258	0.2928	1.1114
1	0.2590	0.3154	0.8895	0.3692	0.3669	1.1030
2	0.1409	0.3829	0.9067	0.2341	0.4237	1.0815
4	0.06635	0.4319	0.9302	0.1361	0.4596	1.0553
∞	0	0.5	1	0	0.5	1

[a]The data are obtained from the electric and magnetic polarizabilities of conducting cylinders calculated by Taylor [40], [41]. $\Sigma(\infty)$ and $\Sigma(-1)$ are the sums $N_{mx} + N_{my} + N_{mz}$ for $\chi \to \infty$ and $\chi = -1$.

electrostatic shielding in a conductor and magnetostatic shielding in the same body but with $\chi \to \infty$.

There is a relation between β_{ll} and α_{tt} [41],

$$\mu_0 \beta_{ll} = -\alpha_{tt}/(2\epsilon_0), \tag{45a}$$

which leads to an exact relation between $N_{mx}(\infty)$ and $N_{mz}(-1)$,

$$N_{mx}(\infty) = N_{my}(\infty) = \tfrac{1}{2}[1 - N_{mz}(-1)]. \tag{45b}$$

Table VI lists $N_{mz}(\infty)$, $N_{mx}(\infty)$, $N_{mz}(-1)$, and $N_{mx}(-1)$ for short cylinders based on the α and β data given by Taylor. From this table we see that the sum of the N_m's deviate from 1 by about 11%. For other values of χ, the deviation should be less, and this could help one estimate N_{mx} for different values of χ and γ.

B. General Rules for N_f and N_m as Functions of χ and γ

We give some general rules for the variation of N_f and N_m with γ and χ based on the tables and figures. (a) For a given χ, both N_f and N_m decrease with increasing γ. This is because the demagnetizing effect is an "end effect," although the demagnetizing fields depend on both end and side surface poles. When γ increases, the effect of cylinder ends on the midplane and the entire volume decreases. (b) When both γ and χ are fixed, $N_m(\gamma, \chi) > N_f(\gamma, \chi)$. That is, the end effect is weaker at the midplane. (c) N_m decreases with increasing χ at any γ. (d) With increasing χ, N_f increases when $\gamma > 1$ and decreases when $\gamma < 1$; there is a region around $\gamma = 1$ where N_f is insensitive to χ. Rules (b), (c), and (d) give the following relation for $N_f(\chi)$ and $N_m(\chi)$ when $\gamma > 1$:

$$N_m(-1) > N_m(0) > N_m(\infty) > N_f(\infty) > N_f(0) > N_f(-1). \tag{46}$$

(e) For $\gamma > 1$, the ratio N_m/N_f increases with increasing γ and decreasing χ. When γ increases from 1 to 10 to 1000, $N_m(0)/N_f(0)$ increases from 1.37 to 8 to 800; $N_m(\infty)/N_f(\infty)$ is smaller and increases from 1.14 to 1.32 to 1.46. (f) The minimum χ for $N_f(\chi) > 0.99N_f(\infty)$ increases with increasing γ. In fluxmetric ferromagnetic measurements, this rule tells us that $N_f(\infty)$ can be used for dM/dH larger than a minimum value that depends on γ. For $\gamma = 10$, 100, and 1000, the minimum values are 200, 5×10^4, and 10^6.

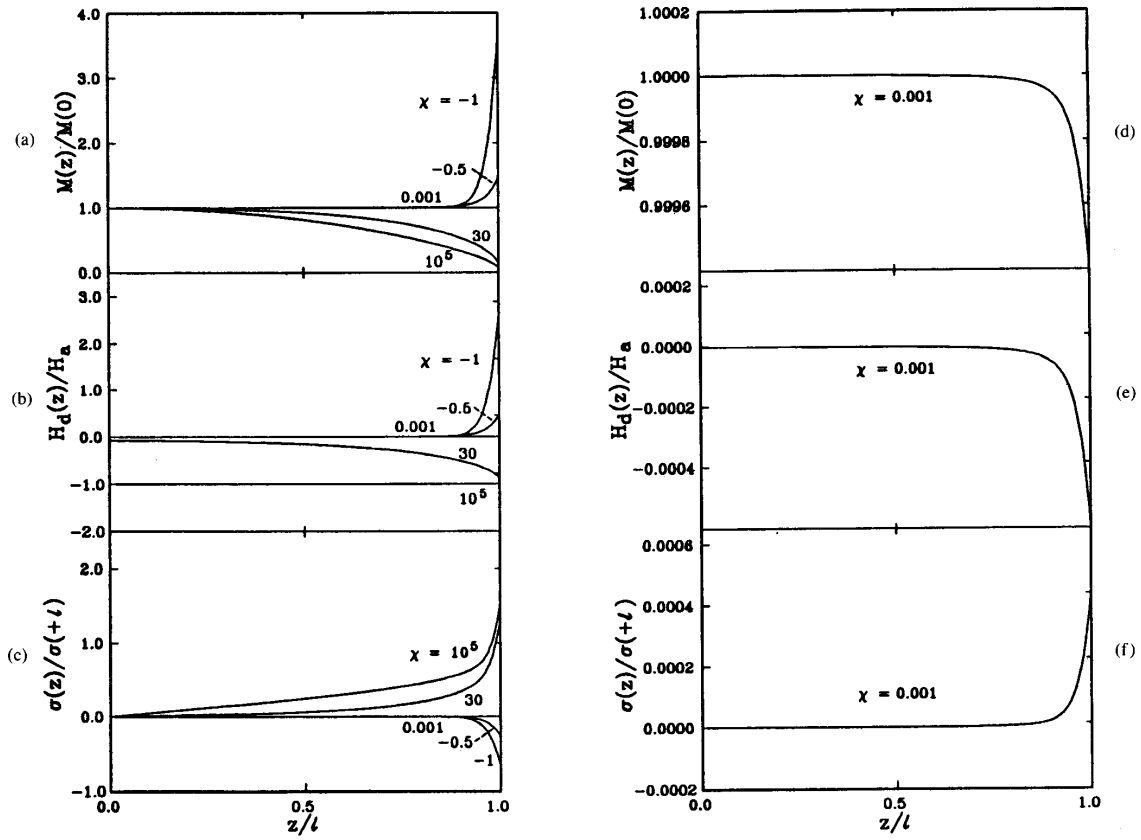

Fig. 8. $M(z)/M(0)$ [graphs (a) and (d)], $H_d(z)/H_a$ [graphs (b) and (e)], and $\sigma(z)/\sigma(+l)$ [graphs (c) and (f)] as functions of z/l for a cylinder with $\gamma = 20$. The curves in graphs (a), (b), and (c) are for $\chi = -1$, -0.5, 0.001, 30, and 10^5, respectively. Graphs (d), (e), and (f) are for $\chi = 0.001$ on an expanded scale.

C. Minimum χ for $N_f(\chi) > 0.99N_f(\infty)$

For $\chi > 0$, the demagnetizing effect resembles the response of an amplifier with negative feedback. The input, output, and gain of the amplifier are H_a, M, and χ, respectively. After operation, M becomes $H_d (H_d = -NM$, where N is the local demagnetizing factor), with sign opposite to that of H_a, which feeds back to the input. The result is that M becomes smaller and nonuniform, while H becomes smaller than H_a. There is perfect feedback when $\chi \to \infty$, and $H = 0$ everywhere. Since $H/H_a = (1 + N\chi)^{-1}$, where N is the local demagnetizing factor, in order to have $N_f(\chi)$ almost equal to $N_f(\infty)$, $(1 + N\chi)$ must be sufficiently large for H/H_a to be small everywhere. Actually N_f is the smallest local N, and the origin of rule (f) may be understood as follows.

$N_f(\infty)$ decreases with increasing γ. To have $N_f(\chi)$ almost equal to $N_f(\infty)$, a smaller $N_f(\infty)$ must be balanced by a larger χ to fulfill the condition of a sufficiently large $(1 + N\chi)$. Therefore, with increasing γ, the minimum χ to satisfy $N_f(\chi) > 0.99N_f(\infty)$ increases. From Table II we can deduce this minimum χ to be $k/N_f(\infty)$ with $15 < k < 17$.

D. Position Dependence of M, H_d, and σ

We have explained rules (a), (b), and (f). To understand the other rules, we have to know the details of the position dependence of M, H_d, and σ. Fig. 8(a), 8(b), and 8(c) gives the curves of $M(z)/M(0)$, $H_d(z)/H_a$, and $\sigma(z)/\sigma(+l)$ as functions of z for $\gamma = 20$ and $\chi = -1$, -0.5, 0.001, 30, and 10^5 computed from the one-dimensional model with $n = 10$. Bloomberg and Arrott [78] derived $M(z)/M(0)$, using a similar approach, for $1 \leq \chi < \infty$ and $\gamma = 100$. Our curves for $\chi = 0.001$ are replotted in Fig. 8(d), 8(e), and 8(f) on finer scales. When H_a is positive, $M(0)$ and $\sigma(+l)$ are positive for $\chi > 0$ and negative for $\chi < 0$. Therefore, for $\chi = -0.5$ and -1, the signs for $M(z)$ and $\sigma(z)$ are opposite to the signs shown for $M(z)/M(0)$ and $\sigma(z)/\sigma(+l)$ in Fig. 8(a) and 8(c). Also, $M(z)$ and $H_d(z)$ are even functions of z, but $\sigma(z)$ is an odd function of z.

E. χ Dependence of N_m/N_f

For $\chi = 10^5$ (that is, $\chi \to \infty$) we can see in Fig. 8(b) that $H_d(z)$ is a constant equal to $-H_a$ in the entire cylinder, which makes H very small (0 for $\chi \to \infty$) and $M(z)$

finite. $M(z)$ is approximately parabolic as shown in Fig. 8(a) and as already pointed out by other authors [21], [27]. The average H_d is equal to $-H_a$. For the midplane and the entire volume, respectively, the average M is $M(0)$ and approximately $0.67M(0)$. Therefore, N_m/N_f should be close to 1.5.

When χ decreases to 30, the variation of $M(z)$ is gradual for small z and sudden in the end regions. This increases the volume-averaged M to more than $0.67M(0)$. But because $H_d(z)$ becomes rather z dependent and its absolute value at $z = l$ is much larger than at $z = 0$ [Fig. 8(b)], N_m/N_f is larger.

As χ decreases to 0.001, both $M(z)$ and $H_d(z)$ remain nearly constant in Fig. 8(a) and 8(b). The reason is that $M(z)$ is very small compared to H_a, so $H_d(z)$ is even smaller than H_a. The variation of the extremely small $H_d(z)$ cannot be seen in Fig. 8(b), and the modification of the field by such a small $H_d(z)$ causes an invisible change in M in Fig. 8(a). However, if we expand the scales [Fig. 8(d) and 8(e)], we can see that the variation of $M(z)$ and $H_d(z)$ continues the trend of decreasing χ from 10^5 to 30. This makes N_m/N_f even larger.

When χ is small but negative, both $M(z)$ and $H_d(z)$ change their signs. At this point, N_f and N_m continue the trend without sudden change. The situation for $\chi < 0$ can be seen from the curves for $\chi = -0.5$ and -1 in Fig. 8(a) and 8(b). For these two cases, $H_d(z)$ and the absolute value of $M(z)$ remain constant until $z > 0.8l$, and then they suddenly increase. This makes N_m/N_f largest when $\chi = -1$. Further discussion of this in terms of pole distribution is given in the next section.

F. χ Dependence of N_f

To understand the susceptibility dependence of N_f for $\gamma > 1$, we focus on the magnetic pole distribution shown in Fig. 8(c) and 8(f). For the largest χ, $\sigma(z)$ varies with z almost linearly on the cylinder surface except for the regions close to the ends. This means that the magnetic poles are the most uniformly distributed on the cylinder, and $H_d(0)$, which has a greater contribution from the poles in the central region than from the ends, is the largest. Thus N_f is its largest for the highest χ.

When χ is decreasing, the variation of $\sigma(z)$ is progressively greater in the end regions, while the magnetic pole density in the central region becomes gradually lower. Therefore, N_f decreases with decreasing χ. When $\chi = 0$, all the poles are at the ends, $\sigma(z)$ is 0, and N_f should be its smallest. In fact, N_f continues to decrease when χ becomes negative. The reason is that, although $\sigma(x)$ remains 0 in a large central region for $\chi < 0$, $\sigma(z)$ for z close to l increases with decreasing χ and its sign is opposite to that of $\sigma(+l)$ [Fig. 8(c)]. The side poles produce a field at the center directed opposite to the field produced by the end poles, so that the demagnetizing effect of the end poles is partially compensated by the effect of the side poles. This makes N_f a little lower than for $\chi = 0$. The side poles close to the ends, with signs opposite to those of the end poles, have a different effect on N_m. They greatly increase the value of H_d in the end regions, so the volume-averaged N_m increases with decreasing χ even for negative χ. Finally, we have the largest value of N_m/N_f at $\chi = -1$.

When $\gamma < 1$, the susceptibility dependence of N_f is the opposite. We can explain this as follows. For oblate cylinders, the end poles are the main contributors to the demagnetizing field H_d at the midplane. For a given $\langle M_z \rangle$ at the midplane, the end-pole density is smallest when $\chi \to \infty$ since, in this case, the poles are the most uniformly distributed on the entire surface. Therefore N_f is the smallest. A smaller positive χ repels the poles to the end regions, which gives rise to a larger end-pole density and a larger N_f. Although all the poles are distributed on the ends when $\chi = 0$, the pole density on the ends is not the largest. This is because, when $\chi < 0$, the end-pole density has a sign opposite to that of the side-pole density nearby, as can be seen from Fig. 4; thus the end poles are further enhanced. As a consequence, the end pole density increases continuously with decreasing χ regardless of its sign, and N_f takes its largest value when $\chi = -1$.

G. Error Transmission in Susceptibility Measurements

From the above analysis we see that, at present, the accuracy of N_m and N_f can reach 1% in general. To know if this accuracy is good enough for the purpose of magnetic measurements, we examine the influence of the error in N_m or N_f on susceptibility measurements. We consider a cylinder consisting of material with constant χ in a longitudinal applied field H_a. An external susceptibility χ_e can be defined as $\langle M \rangle / H_a$, where the average is taken over the whole volume or the midplane, depending on whether N_m or N_f is considered. From (3), replacing N by $N_{f,m}$ and M by $\langle M \rangle$, we obtain

$$\chi = \chi_e(1 - N_{f,m}\chi_e)^{-1}. \tag{47}$$

This equation is accurate under the above assumptions and definitions. From (47), the relative error in χ caused by the calculation error of $N_{f,m}$ and the measurement error of χ_e can be derived as

$$|\Delta\chi/\chi| = |N_{f,m}\chi|\,|\Delta N_{f,m}/N_{f,m}| + (\chi/\chi_e)|\Delta\chi_e/\chi_e|. \tag{48}$$

On the right-hand side of (48), the first term is the transmission error from the erroneous $N_{f,m}$ calculation to the χ determination. This error equals the error in $N_{f,m}$ multiplied by a factor $\alpha_1 \equiv |N_{f,m}\chi|$, which can be obtained from the results of this work. We examine three typical cases. In the first case, $|\chi|$ and α_1 are small; the error in $N_{f,m}$ can be large and still result in a small transmission error. For example, when $|\chi| = 0.1$, we have $\alpha_1 < 0.1$ since $N_{f,m} < 1$, and less than 10% of the $N_{f,m}$ error is reflected in the final χ result. The second case is a magnetometric measurement for $\chi = -1$. α_1, obtained from Table V, is 0.37, 0.17, and 0.06 for $\gamma = 1$, 3, and 10; only a small part of the error in N_m is transmitted to the final χ result. In the third case, high-χ materials are considered. To reduce the error due to the large α_1, flux-metric measurements should be made with long samples, since $N_f < N_m$ and N_f decreases with increasing γ. To

ensure that $\alpha_1 < 1$ based on Table II and Fig. 2, γ should be 12, 58, 200, and 700, for $\chi = 10^2$, 10^3, 10^4, and 10^5, respectively.

The second term in (48) is the transmission error due to the measurement error of χ_e. The corresponding factor is $\alpha_2 \equiv \chi/\chi_e$. For the first case where α_1 is very small, α_2 is very close to 1 since $\chi \simeq \chi_e$, so the error in χ is almost the same as the χ_e measurement error. For our second case, from (47), we have $\alpha_1 + \alpha_2 = 1$. This is interesting because, when γ is small so that $N_m \to 1$ and $\alpha_1 \to 1$, the χ error is mainly due to the error in N_m, no matter how large the χ_e measurement error is. For the high-χ case, if $\alpha_1 = 1$, we have $\alpha_2 = 2$ from (47), leading to a double transmission error to χ from the χ_e measuring error. As a consequence, to obtain accurate results of χ for high-χ materials, both accurate N_f and accurate χ_e are strongly required if γ cannot be made very large.

In summary, to determine χ accurately, the higher the $|\chi|$ of the material, the higher is the required calculation accuracy of $N_{f,m}$. From a magnetic measurement point of view, our calculation accuracy for $N_{f,m}$ at $\chi = 0$ is more than adequate, and the number of calculated points is sufficient for accurate interpolation over a wide range of values. For other χ values, the requirement for calculation accuracy will be determined by the particular purpose of the magnetic measurement; a 1% accuracy may be sufficient for many uses but is inadequate for others. For example, our 0.2% accuracy for $\chi = -1$ is required for superconductor calibration standards.

H. Application to Materials with $\chi > 0$

Most materials have $\chi > 0$, and our results can be used for demagnetization corrections of their magnetic measurements. For materials with linear or nearly linear magnetization curves, our $N_{f,m}$ values are satisfactory. These include paramagnets, spin glasses, weakly magnetic materials, and iron-powder cores and ordinary ferromagnets in the initial and saturation states. However, even in these cases, some caution is required. We give an example below.

For magnetometric measurements of weakly magnetic materials ($\chi < 0.01$) only very small demagnetizing corrections are needed. However, such materials can also be measured by fluxmetric methods, as recommended by at least one measurement standard [79]. A source of error in fluxmetric measurements is if the sample diameter is less than that of the measurement coil. A large demagnetizing effect would occur in the measurement of M because the measured flux linkage is contributed not only by the M of the sample but also by the H_d within the coil volume produced by the sample's poles. Furthermore, fluxmetric measurements on weakly magnetic materials require many coil turns, which ensures that this error will arise. The error in χ due to this effect can be as large as 30%, even if the requirements of [79] are followed [38], [64].

The magnetization curves of ferromagnetic materials are nonlinear, and it is difficult to assign to them specific χ and $N_{f,m}(\chi)$ values except in the initial state and when approaching saturation, as mentioned above. However, our results can still be used satisfactorily for long magnetically soft materials over a wide field range. We can regard χ as the normal susceptibility $\chi_n = M_m/H_m$, where the subscript m denotes the maximum value at the endpoints of a symmetric magnetization loop, and use $N_f(\chi)$. To extract an unknown χ from fluxmetric measurements of χ_e on samples with known γ, one uses N_f. But a knowledge of χ is required to select the appropriate N_f value. The known χ_e and γ and the unknown χ and N_f are related by (47) and Table II or Fig. 2, so the unknowns can be calculated simultaneously. An iterative process may be used. N_f is estimated based on the measured χ_e using Table II or Fig. 2, and χ is calculated from χ_e and N_f using (47). Then a better estimate of N_f is made. Since the differential susceptibility is field dependent in ferromagnets, this treatment involves some error. The resultant χ is an effective susceptibility χ_{eff}. Its value is between χ_n and an averaged differential susceptibility in the sample. We have $\chi_{\text{eff}} = \chi_n$ when $H_m \to 0$ or $H_m \to \infty$, or when the sample has very large γ and χ_n and H_m is close to $H_m(\chi_{n,\max})$. In other cases, including the use of N_m and Tables IV and V, the resultant χ_{eff} may be larger or smaller than χ_n, depending on the measurement conditions.

For measurements of semihard ferromagnets with intrinsic coercivity H_c, Zijlstra [58] has suggested a simple method to obtain a reasonably accurate loop in which the demagnetizing corrections for M and H are performed using $N_f(0)$ and $N_f(\infty)$, respectively. With our results, nonzero finite effective χ (corresponding to the differential susceptibilities at $H = H_c$ and $H = H_m$) can be used more properly.

I. Remarks Concerning $\chi < 0$ and Nonuniform χ

For normal diamagnetic materials with uniform χ, values of $N_m(\chi = 0)$ are more than adequate for experimental work. However, large negative values of χ arise in ac magnetic measurements of normal conductors and both ac and dc measurements of superconductors, where bulk magnetic moments have their source in eddy currents and shielding supercurrents, respectively. These magnetic moments allow us to ascribe values of M, H, and χ to these materials.

In an ideal type-I superconductor, $\chi = -1$ because B and the permeability $\mu_0(1 + \chi)$ both equal 0 at every point in the material. The same applies to a normal conductor in an ac field when the skin depth is negligible compared to its dimensions. Thus there is an equivalence between these cylinders and a normal perfectly diamagnetic cylinder. For these cases, our values of $N_m(\chi = -1)$ and $N_f(\chi = -1)$ can be used. We have verified this experimentally with a magnetometric low-field ac susceptibility measurement of a niobium cylinder ($\gamma = 1.033$) below the critical temperature. The susceptometer was calibrated using the known demagnetizing factor and dipole field of a superconducting niobium sphere [80]. We accounted for a 0.4% volume decrease of both the standard sphere and the sample cylinder upon cooling to 4 K, and deduced a value of N_m equal to 0.361 ± 0.001 from (47), with the uncertainty based on the measured scatter in χ_e.

Our two-dimensional calculations give 0.3622. Thus we see that cylindrical superconducting standards for magnetic measurements for use at low fields and temperatures can be made using accurate values of $N_m(-1)$.

The results of this work have to be used more carefully for materials that do not have constant susceptibility. In these cases, an effective susceptibility should be found. For example, the $M(H)$ curve of an ideal type-II superconductor in fields below the lower critical field H_{c1} is linear, with $\chi = -1$. In the mixed state, $M(H)$ increases when $H > H_{c1}$ and the effective χ should be close to the differential susceptibility at each point, which is positive. This causes a discontinuity in the value of N_m above H_{c1}, and a proper demagnetizing correction should take account of this effect. Similar caveats apply to the intermediate state of superconductors.

Normal conducting cylinders in ac fields have $M(H)$ loops, and a complex susceptibility with a negative real part can be defined [81]. However, this susceptibility is due to eddy currents constrained by the skin effect, different from our model assumption of uniform susceptibility. $N_{f,m}$ for $\chi = -1$ may be used in the limit of small skin depth. Otherwise, to obtain good results, γ must be large enough so that only a small correction is needed; our $N_{f,m}$ values for an effective $\chi < 0$ can be used. A similar case arises in hard superconductors, where a portion of the magnetization comes from penetrated supercurrents that follow the critical-state model [82].

Since most cases of magnetic measurements involve nonlinear magnetization curves, the demagnetizing correction using the factors calculated for constant χ should be made cautiously. For this, a deep understanding of the magnetization process and the demagnetizing effect is most important.

Appendix

The demagnetizing field produced by a ring-shaped distribution of magnetic poles is calculated below. Results are presented both for the case where a ring has a finite width, as on the end-plane of a cylinder, or a finite height, as on the side surface of a cylinder. The method follows that of Gray [83], who calculated the field produced by a disk of charge. The pole density is taken to be uniform over the width or height of the ring.

The magnetic scalar potential at a point (r_i, z_i) produced by a pole density σ on the jth ring is given by

$$\Phi_e = (\sigma/4\pi\mu_0) \int_0^{2\pi} \int_{r_1}^{r_2} r_j[(z_j - z_i)^2 + r_j^2 + r_i^2 - 2r_i r_j \cos\phi]^{-1/2}\, dr_j\, d\phi, \quad \text{(A1)}$$

$$\Phi_s = (\sigma a/4\pi\mu_0) \int_0^{2\pi} \int_{z_1}^{z_2} [(z_j - z_i)^2 + a^2 + r_i^2 - 2r_i a \cos\phi]^{-1/2}\, dz_j\, d\phi, \quad \text{(A2)}$$

where Φ_e and Φ_s represent the potential due to a ring on the end-plane and side surface, respectively. The parameters r_1 and r_2 are the inner and outer radii of the ring of poles on the end surface, and z_1 and z_2 are the limits in the z direction of the ring on the side surface. The limits of integration are changed to give

$$\Phi_e = \int_0^{r_2} F(r, \phi)\, dr\, d\phi - \int_0^{r_1} F(r, \phi)\, dr\, d\phi, \quad \text{(A3)}$$

$$\Phi_s = \int_0^{z_2} G(z, \phi)\, dz\, d\phi - \int_0^{z_1} G(z, \phi)\, dz\, d\phi, \quad \text{(A4)}$$

where $F(r, \phi)$ and $G(z, \phi)$ represent the integrands in (A1) and (A2). The definite integral $\int F(r, \phi)\, dr\, d\phi$ has been evaluated by Gray [83]. Using a similar method, we evaluate the other integrals with the results,

$$\int_0^{r_2} F(r, \phi)\, dr\, d\phi = (\sigma r_2/2\mu_0) \int_0^{\infty} \exp(-\lambda|z_j - z_i|) \cdot \lambda^{-1} J_1(\lambda r_2) J_0(\lambda r_i)\, d\lambda, \quad \text{(A5)}$$

$$\int_0^{z_2} G(z, \phi)\, dz\, d\phi = (\sigma a/2\mu_0) \int_0^{\infty} [\exp(\lambda|z_i|) - \exp(-\lambda|z_2 - z_i|)]\lambda^{-1} J_0(\lambda a) J_0(\lambda r_i)\, d\lambda, \quad \text{(A6)}$$

where J_0 and J_1 are Bessel functions and $2a$ is the diameter of the cylinder. Similar expressions where the limits of integration are r_1 and z_1 are obtained from the previous expressions by replacing r_2 with r_1 and z_2 with z_1.

The interaction constants N_z^{ij} and N_r^{ij} are defined for rings on the ends as

$$N_z^{ij} = (\mu_0/\sigma)\, \partial\Phi_e/\partial z_i = f_{2z}^e - f_{1z}^e = [z_j/(2|z_j|)] \left[r_2 \int_0^{\infty} \exp(-\lambda|z_j|) J_1(\lambda r_2) J_0(\lambda r_i)\, d\lambda - r_1 \int_0^{\infty} \exp(-\lambda|z_j|) J_1(\lambda r_1) J_0(\lambda r_i)\, d\lambda \right], \quad \text{(A7)}$$

$$N_r^{ij} = (\mu_0/\sigma)\, \partial\Phi_e/\partial r_i = f_{2r}^e - f_{1r}^e = -\tfrac{1}{2} \left[r_2 \int_0^{\infty} \exp(-\lambda|z_j|) J_1(\lambda r_2) J_1(\lambda r_i)\, d\lambda - r_1 \int_0^{\infty} \exp(-\lambda|z_j|) J_1(\lambda r_1) J_1(\lambda r_i)\, d\lambda \right], \quad \text{(A8)}$$

and, for rings on the side surface, as

$$N_z^{ij} = (\mu_0/\sigma)\, \partial\Phi_s/\partial z_i = f_{2z}^s - f_{1z}^s \quad \text{(A9)}$$

$$= -\tfrac{1}{2} \left[a \int_0^{\infty} \exp(-\lambda|z_2|) J_0(\lambda a) J_0(\lambda r_i)\, d\lambda - a \int_0^{\infty} \exp(-\lambda|z_1|) J_0(\lambda a) J_0(\lambda r_i)\, d\lambda \right], \quad \text{(A10)}$$

$$N_r^{ij} = (\mu_0/\sigma)\,\partial\Phi_s/\partial r_i = f_{2r}^s - f_{1r}^s$$
$$= [z_2/(2|z_2|)]\,a\int_0^\infty \exp(-\lambda|z_2|)J_0(\lambda a)J_1(\lambda r_i)\,d\lambda$$
$$- [z_1/(2|z_1|)]\,a\int_0^\infty \exp(-\lambda|z_1|)J_0(\lambda a)J_1(\lambda r_i)\,d\lambda. \quad \text{(A11)}$$

We have arbitrarily set $z_i = 0$ for ease of notation and have included the factor $z_j/|z_j|$ when needed to account for the sign reversal that occurs when $z_j < z_i$. The integrals in the f factors are given in [84] and reduce to

$$f_{2z}^e = \{-k_2|z_j|[4\pi(a_2b_2)^{1/2}]^{-1}F(k_2) - (2\pi)^{-1}\Lambda(\alpha_2,\beta_2) + \tfrac{1}{2}\}z_j/|z_j| \quad (a_2 > b_2), \quad \text{(A12a)}$$

$$f_{2z}^e = [-k_2|z_j|(4\pi a_2)^{-1}F(k_2) + \tfrac{1}{4}]z_j/|z_j| \quad (a_2 = b_2), \quad \text{(A12b)}$$

$$f_{2z}^e = \{-k_2|z_j|[4\pi(a_2b_2)^{1/2}]^{-1}F(k_2) + (2\pi)^{-1}\Lambda(\alpha_2,\beta_2)\}z_j/|z_j| \quad (a_2 < b_2), \quad \text{(A12c)}$$

$$f_{2r}^e = -(a_2/b_2)^{1/2}(\pi k_2)^{-1}[(1 - k_2^2/2)F(k_2) - E(k_2)], \quad \text{(A13)}$$

$$f_{2z}^s = -k_2(a_2/b_2)^{1/2}(2\pi)^{-1}F(k_2), \quad \text{(A14)}$$

where $a_2 = r_2$ and $b_2 = r_i$, and

$$f_{2r}^s = [-k_2|z_2|b_2(4\pi a_2^2)^{-1}F(k_2) + b_2(4a_2)^{-1}]z_2/|z_2| \quad (a_2 = b_2), \quad \text{(A15a)}$$

$$f_{2r}^s = \{-k_2|z_2|b_2[4\pi a_2(a_2b_2)^{1/2}]^{-1}F(k_2) + b_2(2\pi a_2)^{-1}\Lambda(\alpha_2,\beta_2)\}z_2/|z_2| \quad (a_2 < b_2), \quad \text{(A15b)}$$

where $a_2 = r_i$ and b_2 is the radius of the cylinder. The factors f_{1z}^e, f_{1r}^e, f_{1z}^s, and f_{1r}^s are given by the same expressions except r_2 is replaced by r_1 and z_2 is replaced by z_1.

For each case $k = 4ab/[(a + b)^2 + z^2]$, and $F(k)$ and $E(k)$ are the complete elliptic integrals of the first and second kind. $\Lambda(\alpha, \beta)$ is related to the Heuman lambda function and is expressed in terms of the elliptic integrals of the third kind, $\Lambda(\alpha, \beta) = (1 - p)^{1/2}(1 - k^2/p)^{1/2}\Pi(\alpha, p, \pi/2)$. The parameters p, α, and β are specified by $p = k^2/[1 - (1 - k^2)\sin^2\beta]$, $k = \sin\alpha$, and $\sin^2\beta = z^2/[(a - b)^2 + z^2]$. The elliptic integrals are evaluated numerically using the procedure given in [85].

ACKNOWLEDGMENT

We thank A. S. Arrott, B.-Z. Li, and S. Shtrikman for helpful comments, A. B. Kos and J. Nogués for assistance in computer programming, and T. W. Petersen for help in preparing the figures.

REFERENCES

[1] G. Chrystal, "Magnetism," in *Encyclopaedia Britannica*, 9th ed., vol. 15, 1883, pp. 219–276.
[2] W. Thomson (Lord Kelvin), *Reprint of Papers on Electrostatics and Magnetism*. London: Macmillan, 1872, pp. 470–471.
[3] F. J. Evans and A. Smith, "On the magnetic character of the armour-plated ships of the Royal Navy, and on the effect on the compass of particular arrangements of iron in a ship," *Phil. Trans. Roy. Soc. London*, vol. 155, pp. 263–323, 1865.
[4] J. Clerk Maxwell, *A Treatise on Electricity and Magnetism*, 3rd ed., vol. 2. Oxford: Clarendon, 1892, pp. 66–73. First published 1873. Reprinted New York: Dover, 1954.
[5] H. A. Rowland, "On magnetic permeability, and the maximum of magnetism of iron, steel, and nickel," *Phil. Mag.*, ser. 4, vol. 46, pp. 140–159, Aug. 1873.
[6] H. A. Rowland, "On the magnetic permeability and maximum of magnetism of nickel and cobalt," *Phil. Mag.*, ser. 4, vol. 48, pp. 321–340, Nov. 1874.
[7] C. R. Mann, "Demagnetization factors for cylinders," *Phys. Rev.*, vol. 3, pp. 359–369, Mar.-Apr. 1896.
[8] J. A. Ewing, "Experimental researches in magnetism," *Phil. Trans. Roy. Soc. London*, vol. 176, pp. 523–640, 1885.
[9] Lord Rayleigh (J. W. Strutt), "I. Notes on magnetism.—On the energy of magnetized iron," *Phil. Mag.*, ser. 5, vol. 22, pp. 175–183, Aug. 1886.
[10] D. Foster, "An experimental method for the determination of the ballistic demagnetization factor," *Phil. Mag.*, ser. 7, vol. 8, pp. 304–313, Sept. 1929.
[11] A. Tanakadaté, "Mean intensity of magnetization of soft iron bars of various lengths in a uniform magnetic field," *Phil. Mag.*, ser. 5, vol. 26, pp. 450–456, Nov. 1888.
[12] H. du Bois, *The Magnetic Circuit in Theory and Practice*, E. Atkinson, translator. London: Longmans, Green, 1896, pp. 23–43.
[13] C. Benedicks, "Ueber die Entmagnetisirungsfactoren kreiscylindrischer Stäbe (Demagnetizing factors of cylindrical rods)," *Ann. Physik*, vol. 6, pp. 726–740, Dec. 1901.
[14] C. L. B. Shuddemagen, "The demagnetizing factors for cylindrical iron rods," *Proc. Amer. Acad. Arts and Sci.*, vol. 43, pp. 185–256, Sept. 1907.
[15] C. L. B. Shuddemagen, "Tables of demagnetizing factors for iron rods," *Phys. Rev.*, vol. 31, pp. 165–169, Aug. 1910.
[16] F. W. Warburton, "The magnetic pole, a useless concept," *Am. Phys. Teacher (Am. J. Phys.)*, vol. 2, pp. 1–6, Feb. 1934.
[17] P. F. W. Preece, "Demagnetizing factors," *School Sci. Rev.*, vol. 52, pp. 309–315, Dec. 1970.
[18] G. Green, *An Essay on the Application of Mathematical Analysis to the Theories of Electricity and Magnetism*. Nottingham, U.K.: Wheelhouse, 1828, pp. 66–72. Reprinted Göteborg, Sweden: Wezäta-Melins Aktiebolag, 1958.
[19] S. P. Thompson and E. W. Moss, "On the self-demagnetizing factor of bar magnets," *Proc. Phys. Soc. London*, vol. 21, pp. 622–633, Dec. 1909.
[20] J. Würschmidt, "Magnetische Anfangspermeabilität, scheinbare Remanenz und Verhalten bei Erschütterungen (Magnetic initial permeability, apparent hysteresis, and behavior under vibration)," *Z. Physik*, vol. 12, pp. 128–164, 1923.
[21] J. Würschmidt, *Theorie des Entmagnetisierungsfaktors und der Scherung von Magnetisierungskurven*. Braunschweig: Sammlung Vieweg, 1925.
[22] H. Neumann and K. Warmuth, "Über die rechnerische Auswertung ballisticher Entmagnetisierungsfaktoren kreiszylindrischer Stäbe (Mathematical evaluation of the ballistic demagnetization factor of circular cylindrical rods)," *Wiss. Veröff. Siemens-Konzern*, vol. 11, pp. 25–35, Jul. 1932.

[23] F. Stäblein and H. Schlechtweg, "Über den Entmagnetisierungsfaktor zylindrischer Stäbe (Demagnetizing factor for cylindrical rods)," *Z. Physik*, vol. 95, pp. 630–646, Jul. 1935.
[24] K. Warmuth, "Die Bestimmung des ballistischen Entmagnetisierungsfaktors mit dem magnetischen Spannungsmesser an Stäben von quadratischem Querschnitt (Determination of ballistic demagnetization factor for specimens of square section)," *Archiv Elektrotechnik*, vol. 30, pp. 761–779, Dec. 1936.
[25] K. Warmuth, "Zur Darstellung des ballistischen Entmagnetisierungsfaktors zylindrischer Stäbe (Ballistic demagnetization factor for cylindrical rods)," *Archiv Elektrotechnik*, vol. 31, pp. 124–130, Feb. 1937.
[26] K. Warmuth, "Über den ballistischen Entmagnetisierungsfaktor zylindrischer Stäbe (Ballistic demagnetization factor of cylindrical rods)," *Archiv Elektrotechnik*, vol. 33, pp. 747–763, Dec. 1939.
[27] R. M. Bozorth and D. M. Chapin, "Demagnetizing factors of rods," *J. Appl. Phys.*, vol. 13, pp. 320–326, May 1942.
[28] R. M. Bozorth, *Ferromagnetism*. Princeton: Van Nostrand, 1951, pp. 845–849.
[29] W. F. Brown, Jr., "Single-domain particles: New uses of old theorems," *Am. J. Phys.*, vol. 28, pp. 542–551, Sept. 1960.
[30] F. W. Grover, *Inductance Calculations*. New York: Van Nostrand, 1946, pp. 142–162.
[31] W. F. Brown, Jr., *Magnetostatic Principles in Ferromagnetism*. Amsterdam: North-Holland, 1962, pp. 187–192.
[32] G. W. Crabtree, "Demagnetizing fields in the de Haas-van Alphen effect," *Phys. Rev. B*, vol. 16, pp. 1117–1125, Aug. 1977.
[33] R. Moskowitz, E. Della Torre, and R. M. M. Chen, "Tabulation of magnetometric demagnetization factors for regular polygonal cylinders," *Proc. IEEE*, vol. 54, p. 1211, Sept. 1966.
[34] J. Kaczér and Z. Klem, "The magnetostatic energy of coaxial cylinders and coils," *Phys. Stat. Sol. A*, vol. 35, pp. 235–242, May 1976.
[35] R. I. Joseph, "Ballistic demagnetizing factor in uniformly magnetized cylinders," *J. Appl. Phys.*, vol. 37, pp. 4639–4643, Dec. 1966.
[36] P. Vallabh Sharma, "Rapid computation of magnetic anomalies and demagnetization effects caused by bodies of arbitrary shape," *Pure Appl. Geophys.*, vol. 64, no. 2, pp. 89–109, 1966.
[37] M. Sato and Y. Ishii, "Simple and approximate expressions of demagnetizing factors of uniformly magnetized rectangular rod and cylinder," *J. Appl. Phys.*, vol. 66, pp. 983–985, Jul. 1989.
[38] D.-X. Chen and B.-Z. Li, "On the error of measurement of feebly magnetic material in regard to demagnetizing field," *Acta Metall. Sinica*, vol. 19, pp. 217–224, Oct. 1983.
[39] D.-X. Chen, *Physical Basis of Magnetic Measurements*. Beijing: China Mechanical Industry, 1985, p. 242.
[40] T. T. Taylor, "Electric polarizability of a short right circular conducting cylinder," *J. Res. Nat. Bur. Standards*, vol. 64B, pp. 135–143, Jul.-Sept. 1960.
[41] T. T. Taylor, "Magnetic polarizability of a short right circular conducting cylinder," *J. Res. Nat. Bur. Standards*, vol. 64B, pp. 199–210, Oct.-Dec. 1960.
[42] W. R. Smythe, "Charged right circular cylinder," *J. Appl. Phys.*, vol. 27, pp. 917–920, Aug. 1956.
[43] W. R. Smythe, "Charged right circular cylinder," *J. Appl. Phys.*, vol. 33, pp. 2966–2967, Oct. 1962.
[44] W. R. Smythe, *Static and Dynamic Electricity*, 3rd ed. New York: McGraw-Hill, 1968, pp. 209–211.
[45] T. L. Templeton and A. S. Arrott, "Magnetostatics of rods and bars of ideally soft ferromagnetic materials," *IEEE Trans. Magn.*, vol. MAG-23, pp. 2650–2652, Sept. 1987.
[46] A. S. Arrott, B. Heinrich, and T. L. Templeton, "Phenomenology of ferromagnetism: I. Effects of magnetostatics on susceptibility," *IEEE Trans. Magn.*, vol. 25, pp. 4364–4373, Nov. 1989.
[47] A. S. Arrott, B. Heinrich, T. L. Templeton, and A. Aharoni, "Micromagnetics of curling configurations in magnetically soft cylinders," *J. Appl. Phys.*, vol. 50, pp. 2387–2389, Mar. 1979.
[48] A. S. Arrott, B. Heinrich, and A. Aharoni, "Point singularities and magnetization reversal in ideally soft ferromagnetic cylinders," *IEEE Trans. Magn.*, vol. MAG-15, pp. 1228–1235, Sept. 1979.
[49] A. Aharoni, "Magnetostatic energy of a saturating cylinder," *J. Appl. Phys.*, vol. 52, pp. 6840–6843, Nov. 1981.
[50] A. Aharoni, "Magnetostatic energy of a ferromagnetic cylinder," *J. Appl. Phys.*, vol. 54, pp. 488–492, Feb. 1983.
[51] W. E. Archer and E. Guancial, "Magnetization distributions in bulk magnetic material," *IEEE Trans. Magn.*, vol. MAG-9, pp. 51–56, Mar. 1973.
[52] T. H. Fawzi, K. F. Ali, and P. E. Burke, "Boundary integral equations analysis of induction devices with rotational symmetry," *IEEE Trans. Magn.*, vol. MAG-19, pp. 36–44, Jan. 1983.
[53] T. Okoshi, "Demagnetizing factors of rods and tubes computed from analog measurements," *J. Appl. Phys.*, vol. 36, pp. 2382–2387, Aug. 1965.
[54] Y. Yamamoto and H. Yamada, "New analytical expressions for flux distribution and demagnetizing factor of cylindrical core," *Electr. Eng. Jpn.*, vol. 102, pp. 1–8, May-Jun. 1982 [*Denki Gakkai Ronbunshi*, vol. 102A, pp. 255–262, May 1982].
[55] R. I. Joseph and E. Schlömann, "Demagnetizing field in nonellipsoidal bodies," *J. Appl. Phys.*, vol. 36, pp. 1579–1593, May 1965.
[56] L. Kraus, "The demagnetization tensor of a cylinder," *Czech. J. Phys. B*, vol. 23, pp. 512–519, May 1973.
[57] J. A. Brug and W. P. Wolf, "Demagnetizing fields in magnetic measurements. I. Thin discs," *J. Appl. Phys.*, vol. 57, pp. 4685–4694, May 1985.
[58] H. Zijlstra, *Experimental Methods in Magnetism*, vol. 2. Amsterdam: North-Holland, 1967, pp. 69–72.
[59] J. A. Osborn, "Demagnetizing factors of the general ellipsoid," *Phys. Rev.*, vol. 67, pp. 351–357, Jun. 1945.
[60] E. C. Stoner, "The demagnetizing factors for ellipsoids," *Phil. Mag.*, ser. 7, vol. 36, pp. 803–821, Dec. 1945.
[61] E. B. Rosa and F. W. Grover, "Formulas and tables for the calculation of mutual and self-inductance," *Bull. Bureau Standards*, vol. 8, pp. 1–237, Jan. 1912, equation (73).
[62] E. B. Rosa and F. W. Grover, "Formulas and tables for the calculation of mutual and self-inductance," *Bull. Bureau Standards*, vol. 8, pp. 1–237, Jan. 1912, equation (54).
[63] L. Cohen, "An exact formula for the mutual inductance of coaxial solenoids," *Bull. Bureau Standards*, vol. 3, pp. 295–303, May 1907.
[64] D.-X. Chen, *Ballistic and Bridge Methods of Magnetic Measurements of Materials*. Beijing: China Metrology, 1990, pp. 77–85.
[65] A. E. Ruehli and D. M. Ellis, "Numerical calculation of magnetic fields in the vicinity of a magnetic body," *IBM J. Res. Develop.*, vol. 15, pp. 478–482, Nov. 1971.
[66] N. Normann and H. H. Mende, "Numerical calculations of the field-dependent magnetization of short rectangular prisms," *Appl. Phys.*, vol. 13, pp. 15–19, May 1977.
[67] C. J. Hegedus, G. Kadar, and E. Della Torre, "Demagnetization matrices for cylindrical bodies," *J. Inst. Math. Its Appl.*, vol. 24, pp. 279–291, Nov. 1979.
[68] G. Kadar, C. J. Hegedus, and E. Della Torre, "Cylindrical demagnetization matrix," *IEEE Trans. Magn.*, vol. MAG-14, pp. 276–277, Jul. 1978.
[69] M. Soinski, "Demagnetization effect of rectangular and ring-shaped samples made of electrical sheets placed in a stationary magnetic field," *IEEE Trans. Instrum. Meas.*, vol. 39, pp. 704–710, Oct. 1990.
[70] T. L. Templeton, A. S. Arrott, and A. Aharoni, "Partially saturated ferromagnetic cylinders," *J. Appl. Phys.*, vol. 55, pp. 2189–2191, Mar. 1984.
[71] W. H. Press, B. P. Flannery, S. A. Teukolsky, and W. T. Vetterling, *Numerical Recipes*. Cambridge, U.K.: Cambridge University Press, 1986, pp. 31–38.
[72] W. F. Brown, Jr. and A. H. Morrish, "Effect of a cavity on a single-domain magnetic particle," *Phys. Rev.*, vol. 105, pp. 1198–1201, Feb. 1957.
[73] W. F. Brown, Jr., *Magnetostatic Principles in Ferromagnetism*. Amsterdam: North-Holland, 1962, pp. 49–53.
[74] R. Moskowitz and E. Della Torre, "Theoretical aspects of demagnetization tensors," *IEEE Trans. Magn.*, vol. MAG-2, pp. 739–744, Dec. 1966.
[75] P. Rhodes and G. Rowlands, "Demagnetising energies of uniformly magnetised rectangular blocks," *Proc. Leeds Phil. Lit. Soc.*, vol. 6, pp. 191–210, Dec. 1954.
[76] E. W. Lee and J. K. Ackers, "A note on the demagnetizing energy of a uniformly magnetized cube," *Brit. J. Appl. Phys.*, vol. 14, pp. 46–47, Jan. 1963.
[77] T. Iwata, "A diagonal sum rule concerning demagnetization tensors in composite bodies," *J. Appl. Phys.*, vol. 39, pp. 3094–3097, Jun. 1986.

[78] D. S. Bloomberg and A. S. Arrott, "Micromagnetics and magnetostatics of an iron single crystal whisker," *Can. J. Phys.*, vol. 53, pp. 1454–1471, Aug. 1975.
[79] American Society for Testing and Materials, "Standard test methods for permeability of feebly magnetic materials," A342-84, *Annual Book of ASTM Standards*, vol. 03.04. Philadelphia: ASTM, 1990, pp. 30–36.
[80] R. B. Goldfarb and J. V. Minervini, "Calibration of ac susceptometer for cylindrical specimens," *Rev. Sci. Instrum.*, vol. 55, pp. 761–764, May 1984.
[81] L. D. Landau, E. M. Lifshitz, and L. P. Pitaevskii, *Electrodynamics of Continuous Media*, 2nd ed. Oxford, U.K.: Pergamon, 1984, pp. 205–207.
[82] C. P. Bean, "Magnetization of high-field superconductors," *Rev. Mod. Phys.*, vol. 36, pp. 31–39, Jan. 1964.
[83] A. Gray, "Notes on electric and magnetic field constants and their expression in terms of Bessel functions and elliptic integrals," *Phil. Mag.*, vol. 38, pp. 201–214, Aug. 1919.
[84] G. Eason, B. Noble, and I. N. Sneddon, "On certain integrals of Lipschitz–Hankel type involving products of Bessel functions," *Phil. Trans. Roy. Soc. London*, vol. A247, pp. 529–551, Apr. 1955.
[85] W. H. Press, B. P. Flannery, S. A. Teukolsky, and W. T. Vetterling, *Numerical Recipes*. Cambridge, U.K.: Cambridge University Press, 1986, pp. 183–190. $\Pi(\pi/2, n, k)$ corresponds to our $\Pi(\alpha, p, \pi/2)$ with $k = \sin\alpha$ and $n = -p$.

Du-Xing Chen was born in Shanghai, China, in 1941. He studied physics at Beijing University from 1958 to 1964, received the M.S. degree from the Institute of Physics, Academia Sinica, in 1981, and received the Ph.D. degree from the Central Iron and Steel Research Institute, Beijing, in 1985.

He is a visiting Professor in the Electromagnetism Group at the Universitat Autònoma de Barcelona, Spain. His areas of research are magnetic measurements, magnetic materials, and superconductor theory and measurements. He was a visiting scientist at the Royal Institute of Technology, Stockholm, from 1985 to 1989, and at the National Institute of Standards and Technology, Boulder, Colorado, during 1988 and 1990. He has published two books entitled *Physical Basis of Magnetic Measurements* (China Mechanical Industry, Beijing, 1985) and *Ballistic and Bridge Methods of Magnetic Measurements of Materials* (China Metrology, Beijing, 1990).

James A. Brug (M'87) was born in Cody, WY, in 1954. He received the B.S. degree in physics from Montana State University and the Ph.D. degree in applied physics from Yale University.

He is currently on leave from Hewlett-Packard Laboratories in Palo Alto, CA, as an ASEE postdoctoral fellow at the National Institute of Standards and Technology in Boulder, Colorado. His research has focused on noise mechanisms in magnetic thin films, measurement of magnetic properties at small length scales, and the magnetics of magnetoresistive recording heads.

Dr. Brug is a member of the American Physical Society.

Ronald B. Goldfarb (M'79–SM'86) was born in Mexico City, Mexico, in 1951. He received the B.A. degree in electrical engineering and the M.S. degree in materials science from Rice University and the M.S. and Ph.D. degrees in physics from Colorado State University.

He is a member of the Superconductor and Magnetic Measurements Group at the National Institute of Standards and Technology (NIST) in Boulder, CO. His areas of research are ac losses and coupling effects in low- and high-temperature superconductors, cryogenic magnetic properties of concentrated spin glasses and weakly magnetic alloys, and magnetic instrument development. From 1979 to 1981 he was a National Research Council postdoctoral research associate at NIST.

Dr. Goldfarb is a member of the American Physical Society and the American Society for Testing and Materials.